

¹ Carbon Dioxide as a Risky Asset

² Adam Michael Bauer^{*1}, Cristian Proistosescu^{2,3}, and Gernot Wagner⁴

³ ¹*Department of Physics, University of Illinois Urbana-Champaign, 1110 W Green St Loomis Laboratory, Urbana, IL
61801, USA*

⁵ ²*Department of Climate, Meteorology, and Atmospheric Sciences, University of Illinois Urbana-Champaign, 1301 W
Green St, Urbana, IL 61801, USA*

⁷ ³*Department of Earth Science and Environmental Change, University of Illinois Urbana-Champaign, 1301 W Green St,
Urbana, IL 61801, USA*

⁹ ⁴*Columbia Business School, 665 W 130th St, New York, NY 10027, USA*

¹⁰ Forthcoming in *Climatic Change*

¹¹ March 13, 2024

¹² **Abstract**

We develop a financial-economic model for carbon pricing with an explicit representation of decision making under risk and uncertainty that is consistent with the Intergovernmental Panel on Climate Change's sixth assessment report. We show that risk associated with high damages in the long term leads to stringent mitigation of carbon dioxide (CO₂) emissions in the near term, and find that this approach provides economic support for stringent warming targets across a variety of specifications. Our results provide insight into how a systematic incorporation of climate-related risk influences optimal emissions abatement pathways.

²¹ **JEL:** G0, G12, Q51, Q54

²² **Keywords:** Climate risk, climate policy, asset pricing, cost of carbon

*Corresponding author email: adammb4@illinois.edu

²³

1 Introduction

24 Climate change's impact on the economy first gained prominence in the economics literature some 30
25 years ago, when the first climate-economic Integrated Assessment Model (IAM) calculated the cost
26 of a marginal ton of carbon dioxide (CO_2) emissions to society, coined the 'Social Cost of Carbon'
27 (SCC) (Nordhaus, 1992). IAMs have since taken center stage in climate policy discussions, with the re-
28 sulting SCC estimates being utilized as benchmarks by companies and governments worldwide (World
29 Bank, 2021). To date the most prominent IAM by far – the dynamic integrated climate-economy,
30 or DICE – evaluates climate change impacts within the context of a standard Ramsey growth econ-
31 omy (Nordhaus, 2017; Barrage and Nordhaus, 2023). In this approach, a global social planner considers
32 tradeoffs between emitting CO_2 and incurring damages both now and, largely, in the future, versus
33 abating CO_2 emissions now at some cost. Performing a benefit-cost analysis results in a presently-low
34 and rising optimal SCC over time, with significant global average warming by 2100. Recent efforts have
35 yielded comparatively higher SCC estimates; Rennert et al. (2022), for example, calculates a central
36 SCC of \$185 but did not explore the optimal control problem of weighing the benefits and costs of
37 abating CO_2 emissions.¹ It is notable that DICE's optimal warming projections are significantly larger
38 than each warming target – 1.5 °C and 2 °C by 2100 – established in the 2015 Paris Agreement. While
39 this inconsistency has called into question the authority of such models in the climate policy discussion
40 to some (Pindyck, 2013; Stern, 2013), DICE has been made consistent with a warming target of 1.5
41 °C with alternative, updated damages and discount rate modules (Hänsel et al., 2020).

42 A limitation of DICE is that it lacks a comprehensive representation of decision-making under risk
43 and uncertainty, a core feature of many 'alternative' climate-economic models (Cai et al., 2016; Cai
44 and Lontzek, 2019; Daniel et al., 2019; Barnett et al., 2020). This is important, as climate change
45 projections are inherently probabilistic, with low probability, extreme impact outcomes presenting the
46 most significant risk to the climate-economic system (Weitzman, 2009). The inherently unpredictable
47 nature of the impacts of climate change has led some to think of climate policy as a form of "insur-
48 ance" to be taken out against high climate damages (Weitzman, 2012). Conventional IAMs do not
49 allow for such considerations in determining their policy projections. Put in financial-economic terms:
50 conventional IAMs do not allow individuals to 'hedge' against climate impacts.

51 To address this, there have been considerable advances in climate-economic modeling that include
52 the effects of risk and uncertainty on the SCC and on optimal policy responses to climate change;
53 see Lemoine and Rudik (2017) for a comprehensive review, while Cai and Lontzek (2019) and Lemoine
54 (2021) represent seminal works for including climate-related risk in IAMs.² We contribute to this
55 extensive literature by introducing the carbon asset pricing model AR6 (CAP6), a climate-economy
56 IAM that builds on previous financial asset pricing climate-economy models (Daniel et al., 2016, 2019).
57 Our paper makes three primary contributions. The first is along methodological lines: we distill each
58 working group report in the sixth assessment report (AR6) issued by the Intergovernmental Panel on
59 Climate Change (IPCC) (Intergovernmental Panel on Climate Change, 2021, 2022a,b) into workable

¹This SCC estimate represents a significant increase from the U.S. Interagency Working Group's central estimate of ~\$50 (Committee on Assessing Approaches to Updating the Social Cost of Carbon et al., 2017) and is in line with the U.S. Environmental Protection Agency's recent draft estimates that report a central value of \$190 (National Center for Energy Economics, 2022).

²We provide a more thorough literature review in Online Appendix A.

60 IAM components.³ This allows our model to be up-to-date with the state-of-the-art calibrations for
61 critical model components. Notably, we formulate a new marginal abatement cost curve (MACC) based
62 on AR6 data, providing an update to the well-known [McKinsey & Company \(2013\)](#) MACC.

63 The second contribution is a computation of optimal carbon prices and associated mitigation policy.
64 Following [Daniel et al. \(2016, 2019\)](#), we embed a representative agent in a binomial, path-dependent
65 tree that allows for risk assessment to endogenously evolve over time. The agent maximizes the Epstein-
66 Zin-Weil utility ([Epstein and Zin, 1989; Weil, 1990; Epstein and Zin, 1991](#)) at every node in the tree
67 such that the present-day utility is maximized. Agent discount rates are calibrated to be in-line with
68 a recent expert elicitation ([Drupp et al., 2018](#)) and the U.S. Environmental Protection Agency (EPA)
69 latest estimates for the SCC ([National Center for Energy Economics, 2022](#)). Notably, we find that the
70 optimal expected warming in our EPA-consistent calibrations is in line with the 2100 warming targets
71 established in the Paris agreement. We find that even if we were pessimistic about the cost of mitigation
72 estimates provided by the IPCC, the EPA-consistent calibration of CAP6 would still support limiting
73 warming to less than 2 °C by 2100, with a discount rate of 2% or lower.⁴

74 In computing optimal mitigation strategies, we capture uncertainty associated with both climate
75 damages and global temperature rise. For damages, we capture both parametric uncertainty inherent
76 to a given damage function, as well as structural uncertainty associated with different damage function
77 shapes; in other words, in addition to Monte Carlo sampling damage levels for a given damage function,
78 we also account for the fact that it is difficult to determine which damage function is correct in the
79 first place ([Pindyck, 2013; Intergovernmental Panel on Climate Change, 2022a](#)). To our knowledge,
80 we are the first to capture this dimension of climate-economic uncertainty. We also account for the
81 marginal damages associated with a probabilistic assessment of climate tipping points ([Lenton et al.,](#)
82 [2008; Dietz et al., 2021](#)).

83 Our final contribution is a sensitivity analysis that allows us to identify how each exogenous as-
84 sumption drives model output. We show that while the expected carbon price depends on the emissions
85 baseline, the expected temperature rise, level of CO₂ concentrations, and incurred economic damages
86 does not. This suggests that our model robustly calculates an economically optimal temperature level
87 for a given calibration; the price of actualizing this temperature level varies across baselines, owing
88 to assumptions about how much emissions are decreasing independently of the policy implemented in
89 CAP6. We find that price uncertainty is dominated by discounting in the near-term and the techno-
90 logical growth rate in the far-term. On the other hand, temperature rise, CO₂ concentration level, and
91 economic damage uncertainty is dominated by discounting for much longer than CO₂ prices, as early
92 inaction leads to warming that cannot be undone later by spending more on abatement (in the absence
93 of significant net-negative emissions or solar geoengineering).

94 We proceed by presenting the socio-economic setup of CAP6 in section 2, the climate emulator in
95 section 3, and our calibration in section 4. We discuss our results in section 5; section 6 concludes.
96 (For section 2, we provide a brief summary paragraph with key equations and figures for readers who

³ [Nielsen-Gammon and Behl \(2021\)](#) highlight the need and urgency for standardized, state-of-the-art climate and economic components based on the most up-to-date research for climate-economic modeling.

⁴This rate is significantly below [Barrage and Nordhaus \(2023\)](#)’s “preferred” rate of 4.5% in 2020, but well within the range that has emerged as a broad consensus among economists ([Council of Economic Advisors, 2017; Drupp et al., 2018; Newell et al., 2022](#)).

97 wish to skip the full technical description of our model components.)

98 2 Socio-economic framework

99 We consider a representative agent with Epstein-Weil-Zin utility given by (2.1), and embed this in-
100 dividual in a binomial tree structure where their utility is maximized. CO₂ emissions (without any
101 agent mitigation action) follow the shared socio-economic projections used by the IPCC (Figure 2).
102 Climate damage functions are calibrated to IPCC working group (WG) II data (see Figure 3) and
103 our uncertainty parameterization captures both epistemic and parametric uncertainty in the damage
104 functions. Finally, we employ (2.12) as our marginal abatement cost curve (Figure 4) and provide
105 two calibrations: our ‘main specification’ based solely on the data in AR6, and the ‘no free lunches’
106 calibration, which excludes negative costs in the AR6 data.

107 2.1 Economic utility

108 CAP6 considers a representative agent with recursive preferences who maximizes their utility through-
109 out time. We choose Epstein-Zin-Weil preferences (Epstein and Zin, 1989; Weil, 1990; Epstein and Zin,
110 1991), henceforth abbreviated as ‘EZ’, because of their unique feature of separating risk across states
111 of time and states of nature. This distinction has been shown to be especially relevant for climate
112 economic studies, where risk considerations across different dimensions are key to the outcome (e.g.,
113 Cai and Lontzek, 2019, among many others). The discrete time utility, U_t , of a representative agent
114 with EZ preferences is given by

$$U_t = \left([1 - \beta] c_t^\rho + \beta [\mathbb{E}_t (U_{t+1}^\alpha)]^{\rho/\alpha} \right)^{1/\rho}, \quad (2.1)$$

115 where $\beta := (1 + \delta)^{-1} > 0$ and $\delta > 0$ is the pure rate of time preference (PRTP), $c_t > 0$ is the
116 consumption at time t , $\rho := 1 - 1/\sigma$ and $\sigma > 0$ is the elasticity of intertemporal substitution (EIS),
117 $\alpha := 1 - \psi$ and $\psi > 0$ is agent risk aversion (RA), and \mathbb{E}_t is the expectation operator at time t . When
118 $\alpha = \rho$ (that is, when $\psi = 1/\sigma$), (2.1) collapses into the von Neumann and Morgenstern (1947) expected
119 utility index. Assuming an exogenous growth rate of consumption $g > 0$, in the final period occurring
120 at time T , the utility is given by

$$U_T = \left[\frac{1 - \beta}{1 - \beta(1 + g)^\rho} \right]^{1/\rho} c_T. \quad (2.2)$$

121 Note that, in the EZ framework, risk aversion across time is parameterized by σ , whereas risk aversion
122 across states of nature is parameterized by ψ .

123 2.1.1 Tree structure

124 Following Daniel et al. (2016, 2019), agent utility in CAP6 is optimized within the structure of a
125 binomial tree, therefore embedding the representative agent in a *finite horizon probability landscape*.

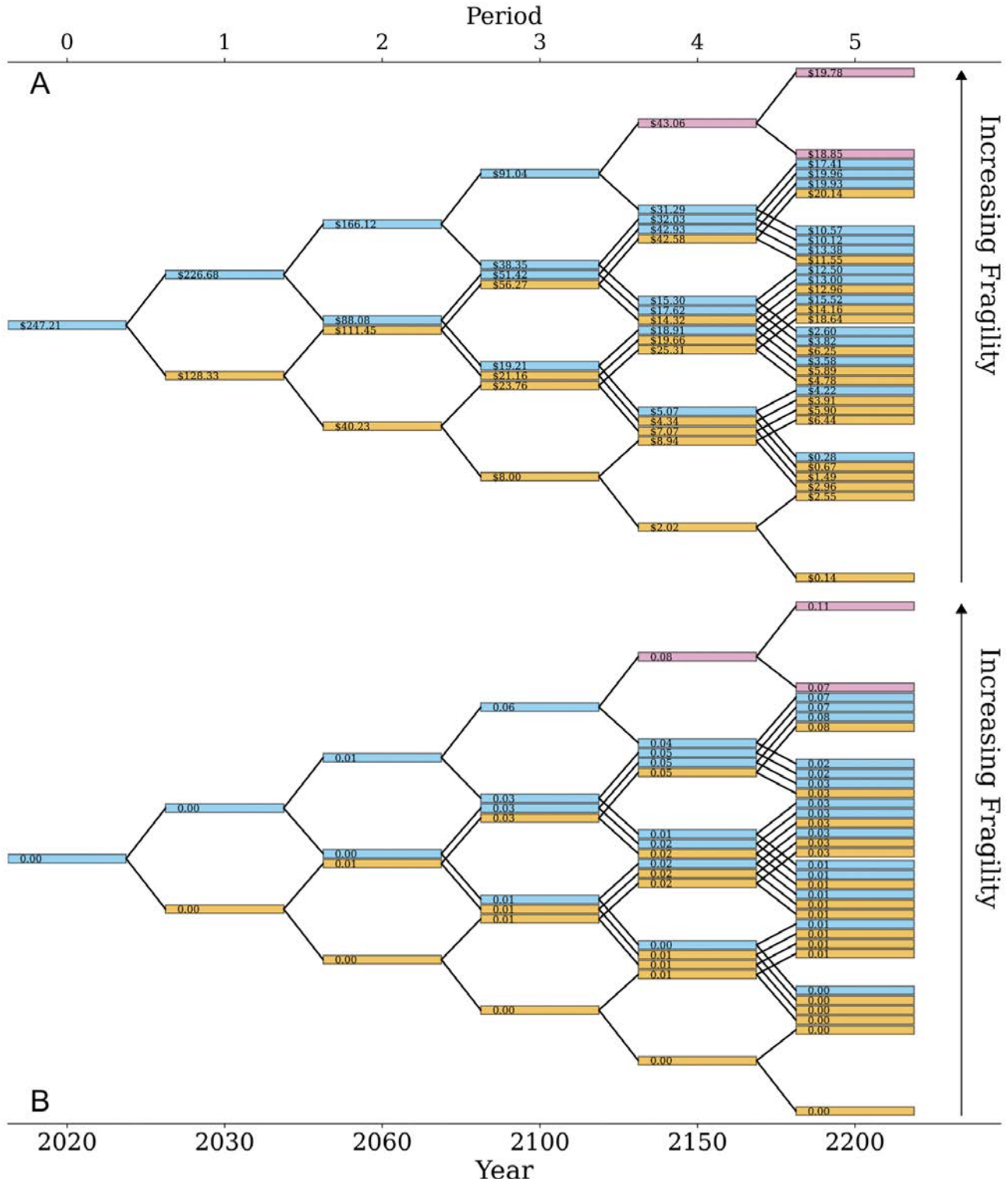


Figure 1: Cost of CO₂ (panel A) and agent experienced climate damages (panel B) at each node. In both panels, we highlight the accessible future states of two agents: one in 2150 (pink boxes) and one in 2030 (gold boxes).

Note: Values are taken from our 2% discount rate featured model run, main specification.

126 This follows a standard approach employed in financial economics ([Cox et al., 1979](#)), and one useful to
127 solve EZ-style models numerically ([Epstein and Zin, 1991](#)).

128 The binomial tree structure of CAP6 is a representation of a time-evolving two dimensional proba-
129 bility distribution of climate damages (see [Figure 1](#) for a schematic). The first dimension is time, while
130 the second is “fragility”, the latter of which encodes the potential for high or low climate damages at a
131 moment in time. Throughout, we will refer to the fragility coordinate at a time t as $\theta_t > 0$. Framing the
132 tree structure as a representation of a two dimensional probability distribution allows for the roles of
133 σ and ψ to be clarified: σ parameterizes risk aversion along the *time* dimension, while ψ parameterizes
134 risk aversion along the “*fragility*” dimension. We choose to orient the fragility coordinate such that
135 high (low, resp.) fragility is associated with high (low, resp.) climate damages. By allowing for many
136 agent decisions, and thus the generation of numerous nodes, we are able to coarsely represent the space
137 of possible fragilities, therefore spanning many possible states of the climate and climate impacts. Note
138 that in the limit of infinitely many decisions, fragility is normally distributed owing to every future
139 state being equally likely, so as to not bias any outcome (be it sanguine or catastrophic) within the
140 model structure.

141 This structure allows for agent risk assessment to evolve endogenously; as an example, consider
142 two agents, one in 2150 and one in 2030 (see [Figure 1](#)). The agent in 2150 has only two future
143 states accessible to them from their position in the tree; this represents an individual who knows well
144 the impact of the climate on the economy. The agent in 2030 has a significantly higher number of
145 future states accessible to them; they know less about how climate change impacts the economy, which
146 influences their decision making, as they have to weigh several possible futures with high and low
147 climate damages (or “fragility”) all at once.

148 This approach has the advantage of being easily computationally tractable, while maintaining a
149 structurally endogenous representation of risk and uncertainty resolution. Moreover, it allows for a
150 transparent interpretation of model results and ample sensitivity analyses, which enables our variance
151 decomposition results in § [5.3.1](#). However, it does suffer from drawbacks: more modern (and computa-
152 tionally expensive and technically challenging) models are able to solve similar optimization problems
153 in continuous-time, on infinite horizons, or both ([Bretschger and Vinogradova, 2014](#); [Cai and Lontzek,](#)
154 [2019](#); [Van Den Bremer and Van Der Ploeg, 2021](#)). These considerations can matter for model results:
155 for example, the time horizon used for climate policy models matters owing to the long residency time
156 of CO₂ in the atmosphere. If one sets the time horizon of the model to 2200, then the net-benefits
157 of a unit of CO₂ abatement in 2190 would matter less than one in 2020 because the benefits would
158 not be given time to materialize. Nevertheless, a number of prominent IAMs used in climate policy
159 consider finite horizons (perhaps most notably, the DICE model is solved on a finite horizon, see [Nord-](#)
160 [haus, 2017](#); [Barrage and Nordhaus, 2023](#)) and our model falls into this class. Moreover, our choice to
161 truncate the time horizon at 2250 aligns with the time where we assume the world reaches net zero
162 emissions without any additional policy in CAP6, which would make, from the policy perspective taken
163 in our model, a carbon tax obsolete (see [Figure 2](#)).

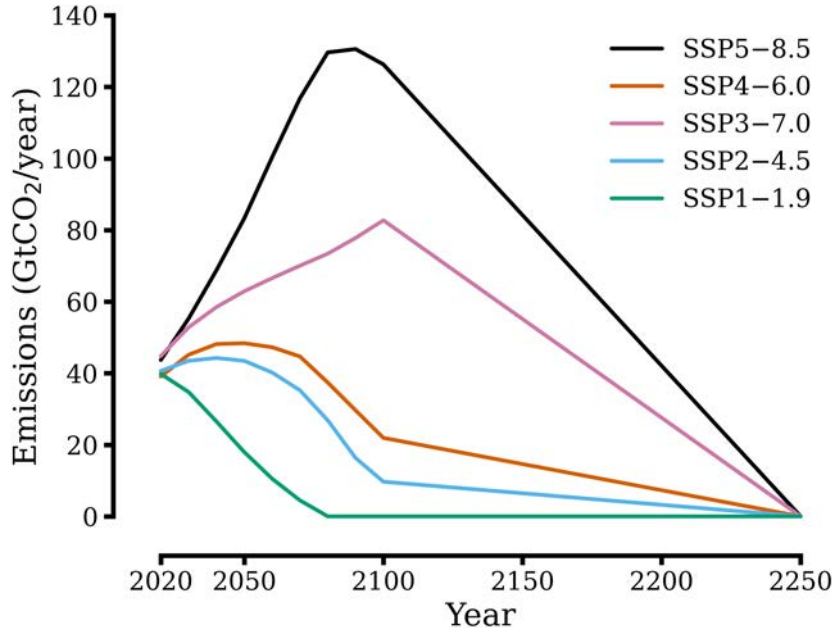


Figure 2: Emissions baselines with their extensions to 2250.

¹⁶⁴ **2.1.2 Statement of utility optimization problem**

Consider a representative agent embedded within a path-dependent binomial tree with T decision periods, leading to $2^T - 1$ total tree nodes. The individual resides within a standard endowment economy (Summers and Zeckhauser, 2008), where at every period time t they are given an amount $\bar{c}_t > 0$ such that $\bar{c}_t = \bar{c}_0(1 + g)^t$. Without loss of generality, set \bar{c}_0 to unity. They cannot consume all of \bar{c}_t , however, owing to both climate change and climate policy. Climate change can cause the agent to lose some amount of \bar{c}_t due to climate damages, $\mathcal{D}_t \geq 0$. Climate policy allows them to spend some amount of \bar{c}_t to reduce their impact on future climate by mitigating some fraction of emissions x_t with total cost κ_t . The consumption of the agent at each time $t \in \{0, 1, 2, \dots, T\}$ is determined by

$$c_0 = \bar{c}_0 (1 - \kappa_0(x_0)), \quad (2.3)$$

$$c_t = \bar{c}_t (1 - \kappa_t(x_t)) (1 - \mathcal{D}_t(\Psi_t, \theta_t)), \quad \text{for } t \in \{1, 2, \dots, T-1\}, \quad (2.4)$$

$$c_T = \bar{c}_T (1 - \mathcal{D}_T(\Psi_T, \theta_T)), \quad (2.5)$$

¹⁶⁵ where Ψ_t is the cumulative CO₂ emissions. We choose $T = 6$ decision periods in all the calculations
¹⁶⁶ in that follow, with our initial and final year being 2020 and 2250, respectively.⁵ The net discounted
¹⁶⁷ EZ-utility is then maximized to obtain the optimal carbon prices and mitigation policies in § 5; see
¹⁶⁸ Online Appendix B for more details on our optimization.

169 **2.2 Emission baselines**

170 There is considerable uncertainty when choosing a ‘business-as-usual’ emissions scenario for climate-
171 economy IAMs ([Hausfather and Peters, 2020](#)). One approach is for the emissions to be a result of
172 economic output (e.g., [Golosov et al., 2014](#)). This approach has the advantage of making the emissions
173 baseline endogenous; however, it also tends to exclude important processes relevant to the level and
174 rate of fossil fuel emissions, such as friction in the diffusion of clean energy technologies, which can be
175 captured by more sophisticated energy systems IAMs.

176 This concern motivates the second approach commonly used by the IPCC, which is to supply a
177 given IAM with a stream of CO₂ emissions exogenously based on plausible future emissions scenarios.
178 The shared socio-economic pathways (SSPs) shown in Figure 2 are an example of this approach,
179 where each baseline represents a “storyline” for future global and regional economic development based
180 on the level of challenges faced by policymakers in mitigation and adaptation. For example, SSP5
181 is a fossil fuel-based development storyline, with high levels of challenge to mitigation (because of
182 significant fossil fuel development) and low challenges to adaptation (because of expanded wealth).
183 SSP1, on the other hand, is a more sustainable route, with low challenges to both mitigation (because of
184 renewable energy expansion) and adaptation (because of equitable growth and investment in education
185 and health). Combining these socio-economic settings with an energy system model produces the
186 emissions projections seen in Figure 2; see [Riahi et al. \(2017\)](#) for a complete review of the SSP storylines
187 and specifics on the underlying assumptions. This approach has been employed by the US Government
188 in their computations of the SCC ([National Center for Energy Economics, 2022](#)),⁶, and is our approach
189 here. This implies that our optimal carbon taxes are always with reference to the emissions baseline
190 we assume; we explore the influence of which emissions baseline we choose on our results in § 5.3.

191 We take emissions data for each SSP at times 2020 – 2100 directly from the SSP database,⁷ and select
192 scenarios which span a range of end-of-century radiative forcing amounts. We make one alteration to
193 the projections provided in the database: negative emissions are set to zero.⁸ As our model extends out
194 to 2250, we require extensions of the SSPs in the database; we follow the prescription of [Meinshausen
195 et al. \(2020\)](#) for each baseline, which assumes that (a) positive fossil fuel emissions and any net-negative
196 fossil fuel emissions are ramped down to zero by 2250, (b) land use CO₂ emissions are zero by 2150, (c)
197 non-fossil fuel greenhouse gas emissions are ramped down by 2250, and (d) land use-related non-CO₂
198 emissions are held constant after 2100. In reality, it is possible that in the absence of a well-designed
199 policy suite that one or more of these assumptions could not hold, which would imply that we are
200 underestimating potential emissions levels in the far-future, and thus long-term climate-economic risk;
201 we explore the relative influence of which emissions baseline we choose in § 5.3. See Figure 2 for the
202 results of our extension procedure.

⁵While one may question the coarseness of our time discretization, it has been shown that including more decision periods in similar models does not significantly affect their output ([Coleman et al., 2021](#)).

⁶Note the US EPA uses the so-called RFF-SPs ([Rennert et al., 2022](#)) rather than the SSPs used here.

⁷See <https://tntcat.iiasa.ac.at/SspDb/dsd?Action=htmlpage&page=10>

⁸This assumption only impacts SSP1–1.9, as SSP1–1.9 makes more optimistic assumptions around backstop technology than we do in our cost formulation.

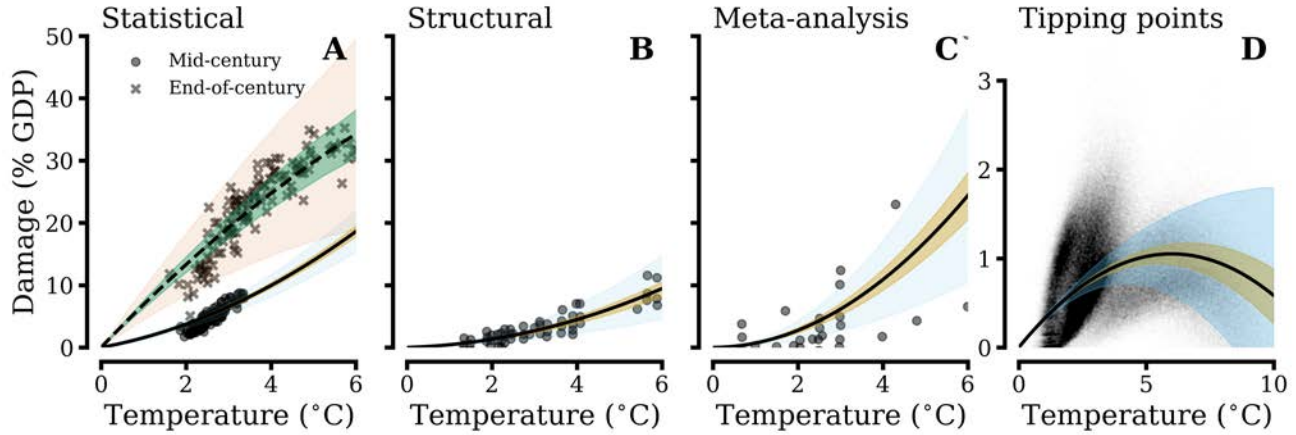


Figure 3: Each of our damage functions by methodology (statistical, structural, and meta-analytic) as well as the marginal damages owing to tipping points.

Note: In each panel, yellow shows ± 1 standard deviation in the damage function, while the blue shaded region shows ± 2 standard deviations. For the end-of-century estimates in panel A, the green region shows ± 1 standard deviation and the salmon shows ± 2 standard deviations. The statistical damage function shown assumes SSP2–4.5.

203 2.3 Damage functions

204 Our climate damage calculation can be broken down into two components: an *aggregate* climate dam-
 205 age, owing to the total damages incurred by climate change, and a marginal *tipping point* climate
 206 damage, which accounts for damages which are incurred by, for example, permafrost melt.

207 2.3.1 Aggregate climate change damages

208 Aggregate damages are defined as global damages owing to climate change, and their magnitude is
 209 estimated in AR6 by WGII ([Intergovernmental Panel on Climate Change, 2022a](#)) (see their Figure
 210 Cross-Working Group Box ECONOMIC.1, panels (a)-(c), p. 16-114). We specify three aggregate
 211 damage functions: one that is modeled after statistical climate damage modeling efforts ([Burke et al.,](#)
 212 [2018](#)), one estimated using structural estimation techniques ([Rose et al., 2017](#)), and a meta-analysis of
 213 climate damage estimates ([Howard and Sterner, 2017](#)), such that for each we have

$$\mathcal{D}(T') = T'(\varpi_1 + \varpi_2 T') \quad (2.6)$$

214 where $\varpi_1, \varpi_2 \in \mathbb{R}^+$ are fitted coefficients. We refer to each of these damage functions by their estimation
 215 methodology in what follows, i.e., “the statistical damage function” and so on. We supply the fitted
 216 coefficients and their uncertainty, as well as a discussion of the qualifications and the limitations of
 217 each individual damage function we use, in Online Appendix D. We present the data and fitted curves
 218 in Figure 3 (ft. ⁹).

⁹We present CAP6 output using only one of each damage function, and compare it to when each damage function is sampled in Online Appendix H.

219 **2.3.2 Tipping point damages**

220 In addition to the aggregate damages accrued owing to climate change, an additional damage potential
221 exists for climate-related tipping points, such as permafrost melt or Amazon dieback. Previous studies
222 parameterize climate tipping points as instantaneous shocks that immediately result in damages (e.g.,
223 Lemoine and Traeger, 2016b); however, this is unrealistic, as the consequences of “hitting a tipping
224 point” will take time to be fully realized (Kopp et al., 2016; Armstrong McKay et al., 2022). This
225 effect was captured by Cai and Lontzek (2019); they found that the presence of climate tipping points
226 significantly increases the social cost of carbon.

227 A recent analysis allows the effect of a given tipping element to be dynamic over time in an IAM,
228 and estimates the marginal damage associated with ten climate tipping points as a function of global
229 average temperature (Dietz et al., 2021). This approach has the advantage of aggregating over the
230 complex dynamic aspects of tipping points and provides a simple “damage function” for marginal
231 damages owing to tipping points. Moreover, this “damage function” implicitly captures the “domino”
232 effect of hitting a tipping point (Lemoine and Traeger, 2016b; Cai et al., 2016) in its damage estimates.
233 However, our use of this approach has the drawback of not capturing aversion to ambiguity surrounding
234 the location of tipping points (Lemoine and Traeger, 2016a), which has been shown to slightly increase
235 the stringency of climate policy. This provides some context to our results, as including the effects of
236 ambiguity aversion to tipping points would increase the resulting carbon price and optimal mitigation
237 level.

238 We take this additional “damage function” owing to tipping points, $\mathcal{D}_{tp}(T')$, from Dietz et al. (2021)
239 (see their Figure 5c), such that the total damages are given by

$$\mathcal{D}_{tot}(T') = \mathcal{D}(T') + \mathcal{D}_{tp}(T'). \quad (2.7)$$

240 Note that $\mathcal{D}_{tp}(T')$ has the same functional form as the aggregate damage function, i.e., Eqn. (2.6). See
241 Figure 3D for a visualization and Table 1 in Online Appendix D for the coefficients of this damage
242 function and corresponding uncertainties.

243 **2.3.3 Sampling damage function uncertainty**

244 We sample uncertainty in the damage function in two ways. The first is by sampling the parametric
245 uncertainty in each damage function; that is, the uncertainty in the values of ϖ_1, ϖ_2 in (2.6). The
246 distributions of ϖ_1, ϖ_2 are assumed Gaussian with mean and variance provided in Online Appendix D,
247 Table 1. The second source of uncertainty in the damage function pertains to which damage function
248 (i.e., statistical, structural, or meta-analytic) we specify in the first place. As the IPCC WGII makes no
249 recommendations in this regard, we assign a hyper-parameter in our simulated climate damages that
250 randomly chooses a damage function, thus sampling epistemic uncertainty in the damage function.
251 This methodology allows us to remain agnostic with respect to which damage function we choose.

252 **2.3.4 Calculating damages at a particular decision node**

253 A representative agent in our model at a given decision node only knows the possible end states which
254 can be accessed from their state. They do not know the exact fragility at their own node, or any θ_t
255 for $t < T$, owing to the inherent uncertainty surrounding both the climate system (such as the precise
256 value of climate sensitivity) and economic impacts (such as damage functions). Owing to the agent not
257 knowing the current fragility, the damages assessed at their decision time are dependent on proxies for
258 the relevant damage variables. The two proxies used in our model is the set of possible end states, Θ
259 (which tells us which end states are accessible) and the cumulative CO₂ emissions, Ψ_t (which tells us
260 approximately how warm the world should be, but does not immediately map to the temperature at
261 time t owing to uncertainty in the climate sensitivity). These two variables in concert give us a basis
262 from which we can interpolate end state climate damages backwards in time to any decision node.
263 Moreover, a continually-updating fragility parameter allows the expectation of future damages to co-
264 evolve with agent decisions about mitigation, therefore making risk assessment endogenous within our
265 modeling structure. We calculate the damage at a given node as a probability-weighted average of the
266 current-period damages accessible to each end node across states of fragility, such that

$$\mathcal{D}_{node}(\Psi_t, \theta_t) = \sum_{\theta_T \in \Theta} P(\theta_T | \theta_t) \mathcal{D}_{tot}(\Psi_t, \theta_t). \quad (2.8)$$

267 **2.4 Cost of mitigation**

268 Calculating the cost of mitigation requires specifying a marginal abatement cost curve (MACC), which
269 relates the price of abatement to the fraction of emissions abated. Such a curve will vary depending on
270 three factors: (1) the current state of emissions mitigation technologies, which in aggregate represent
271 the abatement potential as a function of cost, (2) the availability of a backstop technology, which
272 allows for net-negative emissions, and (3) technological advancement, which makes mitigation costs
273 cheaper over time ([Gillingham and Stock, 2018](#)). We discuss the limitations to our approach in Online
274 Appendix E.

275 **2.4.1 Marginal abatement cost curve estimation**

276 Estimating MACCs requires a functional relationship between the fraction of emissions abated, x , the
277 per-ton tax rate, τ , and the emission pathway, E . We use the most recent estimates for the cost
278 of CO₂ emission abatement presented in AR6 WGIII ([Intergovernmental Panel on Climate Change,](#)
279 [2022b](#)) (see their Figure SPM.7, p. SPM-50). We make four important assumptions in interpreting the
280 data from AR6 WGIII. First, we assume cost estimates are additive, which is not necessarily the case;
281 however, we expect changes in costs and abatement potential to be small enough to consider them as
282 negligible in this study. Second, we neglect negative costs; that is, whenever WGIII data dictates that
283 costs are < \$0, we set the cost to zero. Third, for abatement potentials outside the range provided
284 by the IPCC, we assume the functional relationship between τ and x established for lower abatement
285 potentials holds. Lastly, we assume that the cost of each option is equal to its maximum cost in its
286 respective range, i.e., the cost of an option in the IPCC \$0–\$20 range is assumed to be \$20. Taken

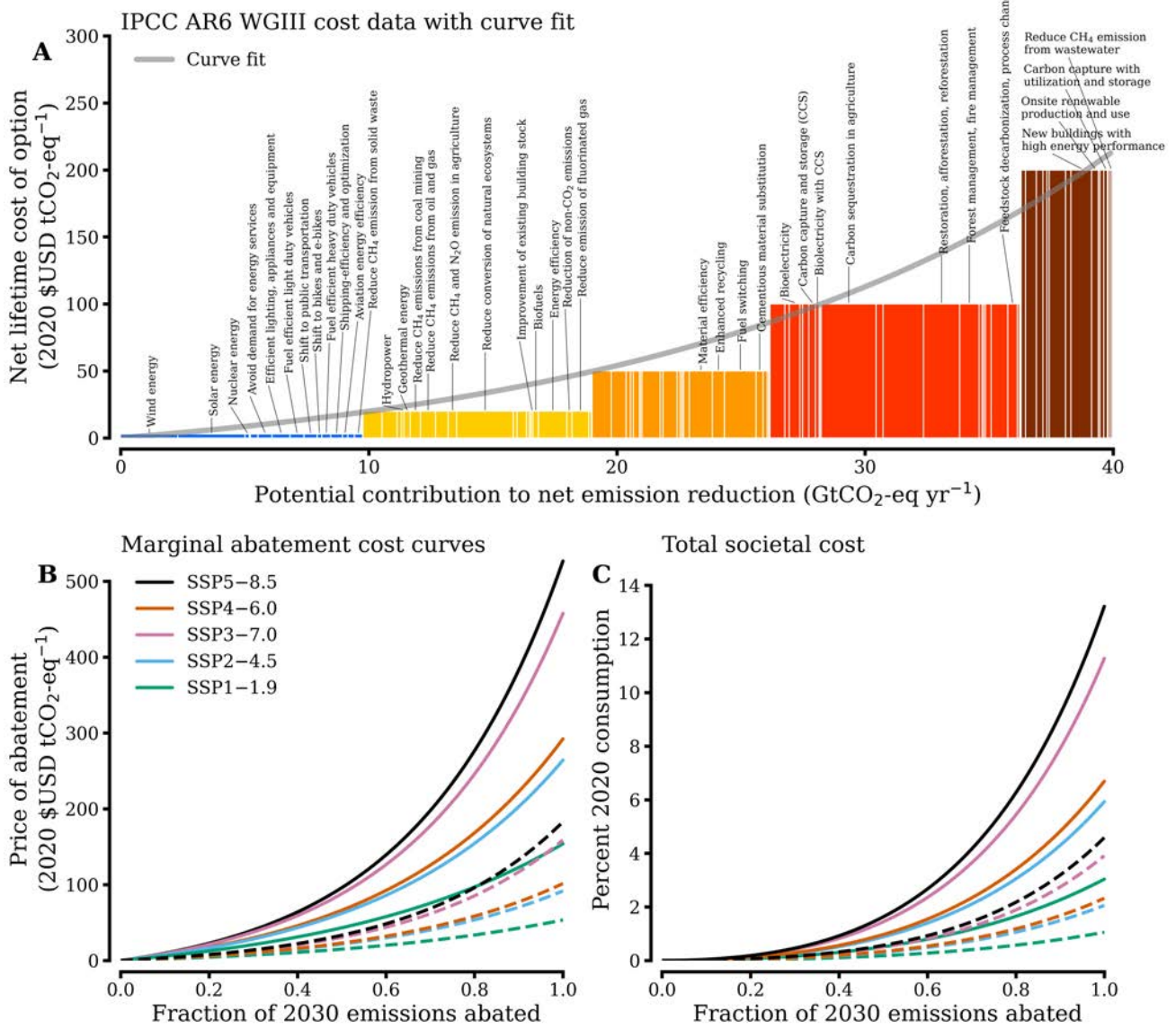


Figure 4: Panel A shows the mitigation potential and cost for each methodology given by the IPCC using their WGIII data. Blue represents zero costs (listed as negative in AR6), yellow is \$0-\$20 range, orange is \$20-\$50, red is \$50-\$100, and maroon is \$100-\$200. Panel B shows the fitted marginal abatement cost curves given by (2.9) and panel C shows the total cost to society given by (2.10) in our ‘main specification’. In panels B–C, solid lines correspond to 2030 MACCs, while dashed lines are 2100 MACCs, assuming an exogenous technological growth rate of 1.5% and no endogenous technological growth.

Note: In panel A, the abatement methodology label is only on the bar with the most mitigation potential for a given methodology.

287 together, these assumptions make our MACC estimation conservative. We then fit an exponential
 288 curve to the cost data (see Figure 4A), such that

$$\tau(x) = \tau_0 \left(e^{\xi x} - 1 \right), \quad (2.9)$$

289 where $\tau_0, \xi > 0$ are constants. To evaluate (2.3)–(2.5), we are interested in the total cost to society,
 290 $\kappa(\tau)$ for each particular tax rate τ , in units of the fraction of 2020 consumption lost. We use the
 291 envelope theorem to calculate $\kappa(\tau)$, such that (see Online Appendix E for the full derivation),

$$\kappa_{MACC}(x) = \frac{E_0 \tau_0}{c_{2020}} \left(\frac{e^{\xi x} - 1}{\xi} - x \right), \quad (2.10)$$

292 where c_{2020} is the 2020 global consumption in billions of 2020 USD, set to \$61880 (taken from the
 293 World Bank¹⁰) and E_0 is the emissions rate in 2030 in GtCO₂ yr⁻¹. A table of fitted values for τ_0 and
 294 ξ for each SSP are provided in Table 3 in Online Appendix E, as well as a calculation for the percent
 295 of consumption required to abate all emissions. Fits for (2.9) and (2.10) are shown in Figure 4B and
 296 Figure 4C, respectively.

297 2.4.2 Direct air capture technology

298 Our model represents direct air capture (DAC) via permitting CO₂ removal (National Research Council,
 299 2015). Net CO₂ removal occurs whenever the mitigation exceeds unity; this leads to negative emissions
 300 and thus net carbon removal from the atmosphere. The price of net carbon removal is a major source
 301 of uncertainty in assessing future climate policy (Johnson et al., 2017), with estimates ranging from
 302 \$50 – \$1000 2020 USD per ton of CO₂ removed. Regardless of the specific dollar estimates provided in
 303 the literature, DAC faces a common hurdle: scalability (Intergovernmental Panel on Climate Change,
 304 2022b). The parameter x in our MACC is the fraction of 2030 emissions abated; therefore, removing
 305 even a small percentage of these emissions from the atmosphere is equivalent to abating billions of tons
 306 of CO₂ from the atmosphere in short order. The technology to carry out this task is simply unavailable
 307 at present, and it is unclear when it will become fully mature and available at scale.

308 Note that, before mitigation reaches unity, there is some carbon capture and storage that is as-
 309 sumed to be occurring concurrent with emissions reductions; indeed, by considering the technology-
 310 by-technology breakdown of the IPCC’s WGIII cost data in Figure 4A, carbon capture and storage
 311 is placed in the \$200 2020 USD tCO₂-eq⁻¹ cost bracket. Hence our inclusion of DAC in our MACC
 312 formulation represents an abrupt shift from purchasing various abatement technologies (such as solar
 313 power or equipment to retrofit buildings) to installing exclusively, and at scale, DAC facilities. The
 314 costs of this process are currently assumed to be rather large (International Energy Agency, 2022).
 315 However, a breakthrough could certainly occur sometime in the future where DAC becomes deployable
 316 at scale for a more economically viable cost (for example, as a result of the uncapped subsidies in the
 317 Inflation Reduction Act of 2022 (Yarmuth, 2022)), which would lower the price of DAC considerably
 318 and would require a reassessment of our quantitative analysis in § 5.

319 In light of these considerations, we take a simple approach to adjusting our cost curve to account

¹⁰<https://data.worldbank.org/indicator/NE.CON.TOTL.CD>

320 for DAC technologies by imposing a DAC premium, $\tau_{DAC} > 0$, which is an extra price for carbon
 321 removal which shifts τ_0 to $\tau_0 \rightarrow \tau_0 + \tau_{DAC}$. Throughout, we essentially price out to-scale DAC leading
 322 to net-negative emissions before 2100. This alters our MACC cost curve (2.10) when $x > 1$, such that

$$\kappa_{MACC}(x) = \begin{cases} \frac{E_0\tau_0}{c_{2020}} \left(\frac{e^{\xi x} - 1}{\xi} - x \right), & 0 \leq x \leq 1, \\ \frac{E_0(\tau_0 + \tau_{DAC})}{c_{2020}} \left(\frac{e^{\xi x} - 1}{\xi} - x \right), & x > 1. \end{cases} \quad (2.11)$$

323 2.4.3 Technological progress

324 Technological progress in CAP6 is captured by allowing the cost of mitigation to society $\kappa_{MACC}(x)$
 325 to decrease in time as technological proficiency makes mitigation cheaper. Technological progress
 326 can occur in two ways: (1) exogenously, where general technological improvement independent of
 327 agent choices make mitigation cheaper, and (2) endogenously, where if a given individual invests in
 328 mitigation early, the cost of mitigation goes down more over time (Acemoglu et al., 2012). The
 329 exogenous (endogenous, resp.) technology advancement rate is given by $\varphi_0 \geq 0$ ($\varphi_1 \geq 0$, resp.).
 330 Incorporating these factors into our cost curve results in our final expression for the cost of mitigation
 331 to society,

$$\kappa_t(x_t) = \kappa_{MACC}(x_t) (1 - \varphi_0 - \varphi_1 X_t)^{t-10}, \quad (2.12)$$

332 where

$$X_t := \frac{\int_0^t x(\zeta) E(\zeta) d\zeta}{\Psi(t)}, \quad (2.13)$$

333 is the weighted average mitigation up to time t (ft. ¹¹).

334 We note that our formulation of endogenous technological change – or “learning by doing” – follows a
 335 formulation akin to Wright’s law (Wright, 1936), where the reduction in costs of mitigation technologies
 336 is proportional to the total deployed mitigation, as opposed to directed technical change in the spirit
 337 of Acemoglu et al. (2012) or Lans Bovenberg and Smulders (1995). This is because in our formulation,
 338 the social planner chooses levels of abatement, which (via proxy) corresponds to the deployment of
 339 clean technologies. As more and more renewable technologies are “deployed” by the planner, Wright’s
 340 law would suggest that their costs will decrease. Hence the Wright’s law-based formulation is the most
 341 natural way to incorporate endogenous technological change into our model. This framework has the
 342 additional advantage of allowing us to only focus on carbon tax levels rather than including additional
 343 policy instruments, such as renewable energy subsidies.

344 2.4.4 “No free lunches” calibration

345 Estimating the cost of CO₂ abatement is notoriously challenging. The cost estimates presented above
 346 are static, in the sense that they represent the costs of the lifetime of the project and, for example, ignore

¹¹Note the technological growth factor is offset by ten years as the cost data from AR6 is for 2030 technologies and our first model period is in 2020.

347 spillover effects ([Intergovernmental Panel on Climate Change, 2022b](#)). However, static estimates fail
 348 to capture the impact of the costs (or savings) associated with a given project that outlive the project
 349 lifetime itself ([Gillingham and Stock, 2018](#)). Such considerations lead some to argue that costs should
 350 not be estimated from the “bottom up” as done here, but rather from the “top down.” “Top down”
 351 estimates generally paint a more pessimistic picture than the “bottom up” methods, positing that the
 352 cost of abating CO₂ emissions is actually larger than adding up the cost of each individual option,
 353 owing to inertia and friction in the economic system, a set of barriers typically summarized as the
 354 “energy paradox” ([Jaffe and Stavins, 1994](#)).

355 To address this concern, we provide an alternative calibration of CAP6 that is more closely aligned
 356 to “top-down” MACCs (see, e.g., [Barrage and Nordhaus, 2023](#)) by adjusting the MACC to exclude
 357 zero-cost abatement technologies; indeed, it has been shown that the degree to which one believes
 358 in zero-cost mitigation explains much of the difference between “top-down” and “bottom-up” MACC
 359 estimates ([Kotchen et al., 2023](#)). We do so by shifting all of the mitigation potential in the IPCC
 360 dataset up by one cost bracket; for example, the zero cost methodologies (the blue bars in Figure 4)
 361 now have \$20 2020 USD tCO₂-eq⁻¹ lifetime cost, and so on. The highest cost abatement technologies
 362 are set to cost \$400 2020 USD tCO₂-eq⁻¹. We coin this MACC calibration as the “no free lunches”
 363 MACC, and provide its parameter values in Online Appendix E, Table 3. (ft. ¹²).

364 3 Climate model

365 Here we present the climate component of our model. We map CO₂ emissions to the temperature
 366 anomaly above preindustrial levels, denoted as T' , using the transient climate response to emissions
 367 (TCRE) ([Damon Matthews et al., 2021](#)). The TCRE is defined as a linear scale factor $\lambda > 0$ that maps
 368 the cumulative CO₂ emissions, $\Psi(t) := \int_0^t E(\zeta)d\zeta$, to temperature, where $E(t)$ is the emissions baseline.
 369 The physical basis for TCRE is a compensation between the diminishing sensitivity of radiative forcing
 370 to CO₂ at higher atmospheric concentration and the diminishing ability of the ocean to take up heat
 371 and carbon at higher cumulative emissions ([Intergovernmental Panel on Climate Change, 2021](#)). We
 372 follow the framework laid out in [Damon Matthews et al. \(2021\)](#) to use a TCRE that accounts for non-
 373 CO₂ forcing via the parameter $f_{nc} > 0$ which increases the average value and variance of the TCRE.
 374 We write our “effective” TCRE – the TCRE including non-CO₂ forcing factors – as

$$\lambda_{eff} := \frac{\lambda}{1 - f_{nc}}. \quad (3.1)$$

375 The mean value of λ , f_{nc} , and λ_{eff} and their uncertainties are provided in Online Appendix F, Table 4.
 376 Using this approach, we are able to reproduce central estimates of warming levels this century reported
 377 by WGI in AR6 for each SSP reasonably well, see Online Appendix F, Table 5. Therefore in our

¹²The analogous figure to Figure 4 for the “no free lunches” MACC is provided in Online Appendix E. We also performed a second recalibration that sets the costs of the the < \$0 mitigation options to infinity, coined the “infinite cost” calibration. The figure associated with this calibration is also in Online Appendix E. We do not show the results of CAP6 with this calibration as the final costs of abatement are lower than in the “no free lunches” case, but higher than the ‘main specification.’ Hence, the results will simply be an interpolation between the main specification and the “no free lunches” results.

378 calculations of temperature, we use

$$T'(t) = \lambda_{eff}\Psi(t). \quad (3.2)$$

379 The TCRE approach has a number of advantages: (i) it captures short- and long-term uncertainty in
380 climate warming, (ii) it is relatively simple and transparent, and (iii) emulates state-of-the-art climate
381 models well (Allen et al., 2009; Dvorak et al., 2022).¹³ Moreover, the TCRE framework has been used
382 in a number of other climate-economic models (e.g., Dietz and Venmans, 2019; Campiglio et al., 2022).

383 4 Model calibration

384 4.1 Featured runs

385 To calibrate CAP6, we use discount rates in line with recommendations from the US government.
386 Previous analyses use a discount rate of 3% (Committee on Assessing Approaches to Updating the
387 Social Cost of Carbon et al., 2017), but recent studies use 2% in light of recent economic trends (such
388 as falling interest rates) and expert elicitation (Council of Economic Advisors, 2017; Drupp et al., 2018).
389 Indeed, New York State adopted a 2% discount rate in their social cost of carbon calculations (New
390 York State Energy Research and Development Authority and Resources for the Future, 2020). We
391 calibrate our featured runs using 1.5%, 2% and 2.5% discount rates to be consistent with the recent
392 report issued by the EPA (National Center for Energy Economics, 2022) and use the term structures
393 from Bauer and Rudebusch (2020). We also show results using a 3% discount rate for consistency with
394 prior US government estimates (Committee on Assessing Approaches to Updating the Social Cost of
395 Carbon et al., 2017).¹⁴ See Online Appendix G, Table 6 for specifics. We assume $g = 1.5\%$ for all
396 runs. For each discount rate, we assume that $\psi = 10$, in line with trends observed in the U.S. financial
397 market (Schroyen and Aarbu, 2017). For our emissions baseline, we choose SSP2–4.5, as it aligns with
398 recent projections of emissions used by the US EPA (Rennert et al., 2022). Lastly, we assume a modest
399 exogenous technological growth rate of 1.5% and no endogenous technological growth, owing to an
400 inability to reliably calibrate the endogenous technological growth rate parameter φ_1 . The choice of
401 no endogenous technological growth makes our technological growth assumptions conservative, given
402 the known link between agent investment in mitigation and rates of growth in clean sectors (Acemoglu
403 et al., 2012).¹⁵

404 4.2 Ensemble runs

405 While risk associated with temperature rise and damage function uncertainty are holistically evaluated
406 in a given run of CAP6, other sources of uncertainty exist and are excluded, such as uncertainty in

¹³Dvorak et al. (2022) showed that the TCRE adequately emulates the response of the more comprehensive FaIR model (Smith et al., 2018), itself a combination of carbon cycle models (Joos et al., 2013) and physical response models (Geoffroy et al., 2013b,a). The TCRE can deviate from more sophisticated models slightly depending on the forcing scenario (Intergovernmental Panel on Climate Change, 2021), but the differences are minor and are therefore ignored in this study.

¹⁴We do not here take a stand on which discount rate is correct, but do consider the 2% rate as our benchmark, as it is the central rate used by the EPA.

¹⁵We demonstrate how including endogenous technological growth influences model output in Online Appendix K.

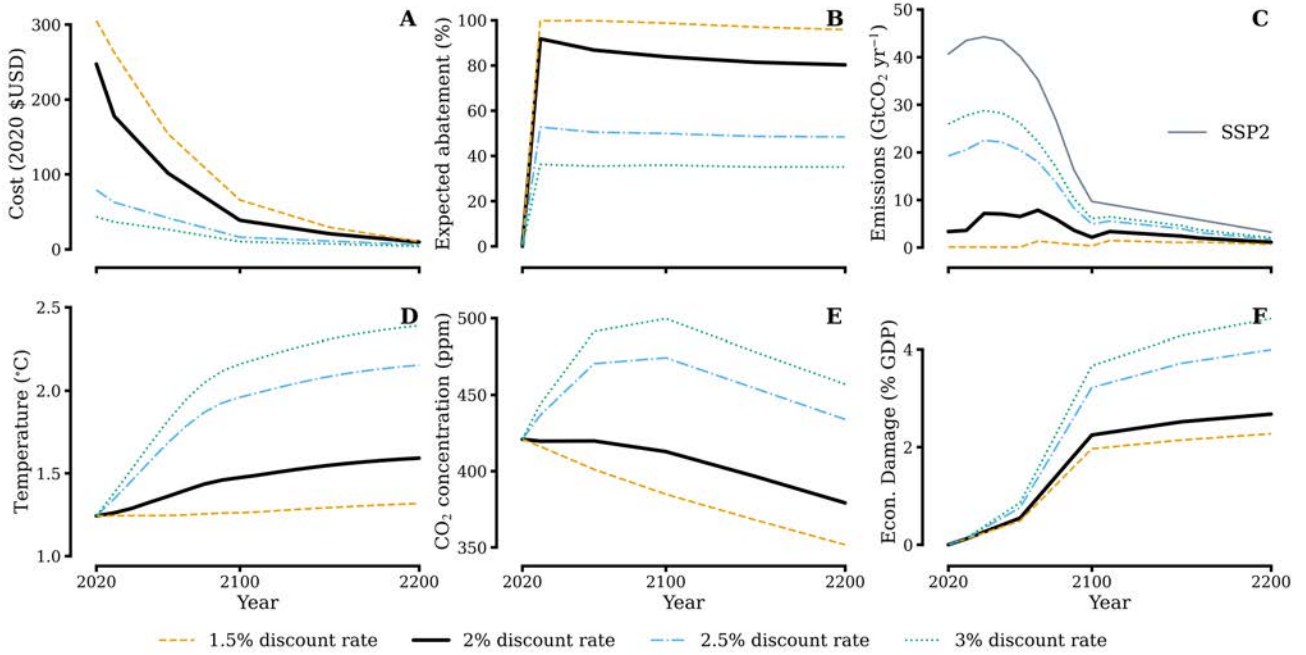


Figure 5: CAP6 output for four discount rates in our main specification.

the rate of technological growth, or which exogenous emissions baseline or discount rate is assumed. Each of these represent a source of epistemic uncertainty in the climate-economic system; indeed, not knowing how much CO_2 will be emitted over the next century, for example, strongly influences the range of possible climate realizations, and thus, climate-related risk (Hawkins and Sutton, 2009; Lehner et al., 2020). To probe the impact of assumptions associated with each of these parameters on model output, we carry out a Monte Carlo analysis. We sample discount rates between the range of 1.5% and 4.25%; we chose the lower bound based on the lower bound considered by the EPA and the upper bound is the preferred rate used in DICE–2016R (Nordhaus, 2017). The value of agent RA has been measured to as high as 15 in wealthy countries and as low as 3 in some European nations (Schroyen and Aarbu, 2017), which defines our range. We choose the modest ranges of 0%–3% for both the exogenous and endogenous rate of technological growth. Note that we use our ‘main specification’ MACC for the ensemble run analysis. See Online Appendix G, Table 7 for our numerical values.

5 Results

5.1 Main specification

We show the featured model runs of CAP6 in Figure 5. We find that the 2% discount rate policy implies a high cost of carbon and stringent abatement policies, see panels 5A–B. The cost of carbon declines over time; this, however, should not be confused with reduced abatement action over time. Rather, the declining dynamics of carbon prices can be entirely attributed to the improved ability to abate CO_2 emissions owing to technological improvements (see Eqn. (2.12)). This set of mitigation actions leads emissions peaking in 2070, with CO_2 concentrations stabilizing before starting to decrease by mid-century. The expected global temperature change resulting from this emissions policy is less

428 than 1.5 °C by 2100 (~ 1.47 °C) and less than 2 °C in 2200 (~ 1.6 °C).

429 Decreasing the discount rate to 1.5% leads to complete and immediate cessation of emissions (see
430 panel 5B), thus maximizing costs and decreasing 2100 (2200, resp.) warming by 0.2 °C (0.3 °C, resp.)
431 in comparison to the 2% run. Larger discount rates relax the stringent abatement policies seen in
432 the 2% and 1.5% discount rate cases. This results in lower costs and less mitigation action, and
433 consequentially, larger warming and damages. We find that both the 2.5% and 3% discount rates
434 warm beyond the warming target of 1.5 °C by 2100 established in the Paris Agreement. Moreover,
435 the 3% discount rate policy exceeds 2 °C warming by 2100, and the 2.5% discount rate policy barely
436 holds temperatures below 2 °C by 2100 (~ 1.96 °C by 2100). In the case of the 2.5% and 3% discount
437 rates, CO₂ concentrations rise before falling as emissions cease.¹⁶ The 2.5% (3%, resp.) discount rate
438 individual also tends to lose $\sim 1\%$ ($\sim 1.4\%$, resp.) more GDP in 2100 and $\sim 1.3\%$ ($\sim 2\%$, resp.) more
439 in 2200 than in the 2% discount rate case, showing the expensive consequences of delayed action in
440 combating climate change.

441 The intuition behind our declining carbon prices can be found in our structural representation of
442 risk. In the early periods of the model, the social planner faces the risk of catastrophic long-term
443 damages if they choose not to abate any CO₂ emissions ($\sim 50\%$ GDP or higher, if the worst-case
444 climate sensitivity and damage function concurrently materialize); this causes the social planner to
445 mitigate aggressively early on to effectively rule out such catastrophic futures from ever materializing.
446 Technological progress then brings down abatement costs over time (especially if learning-by-doing
447 effects are considered, see Online Appendix K), and drives down the carbon price over time. These
448 two factors combine to cause carbon prices to start high and decline over time.

449 From this analysis, we find that modeling the cost of climate risk with CAP6 supports stringent
450 mitigation action. We find that the carbon price and corresponding mitigation policy associated with
451 the 2% discount rate saves at least \$22 trillion 2020 USD globally in 2100 (assuming global GDP grows
452 annually by 4%) in comparison to the higher discount rate policies. In addition, employing policies
453 with discount rates considered by the EPA result in an expected warming level in line with the targets
454 set forth in the Paris agreement (United Nations Framework Convention on Climate Change, 2015),
455 providing the targets with explicit economic support. When faced with potentially severe damages, the
456 representative agent makes a clear choice: they sacrifice consumption today to abate CO₂ emissions,
457 consistent with our understanding of how risk influences climate mitigation policy.

458 5.2 Alternative calibration: “no free lunches”

459 We recalculate our featured runs using the “no free lunches” MACC and show the results in Figure 6.
460 The “no free lunches” cost curve leads to an increase in the optimal price of carbon; the 2020 CO₂ price
461 increases by 20% in the 2% discount rate case. However, the “no free lunches” MACC significantly
462 influences the efficacy of the optimal price in abating CO₂ emissions. For example, the 2% discount
463 rate policy now abates only 70% of emissions (as opposed to $\sim 85\%$ in the main specification). This
464 emissions pathway reaches ~ 1.7 °C of warming by 2100 and ~ 1.9 °C warming by 2200, notably

¹⁶We use the carbon cycle model of Joos et al. (2013) to compute carbon concentrations for our optimal mitigation pathways, see Online Appendix F.

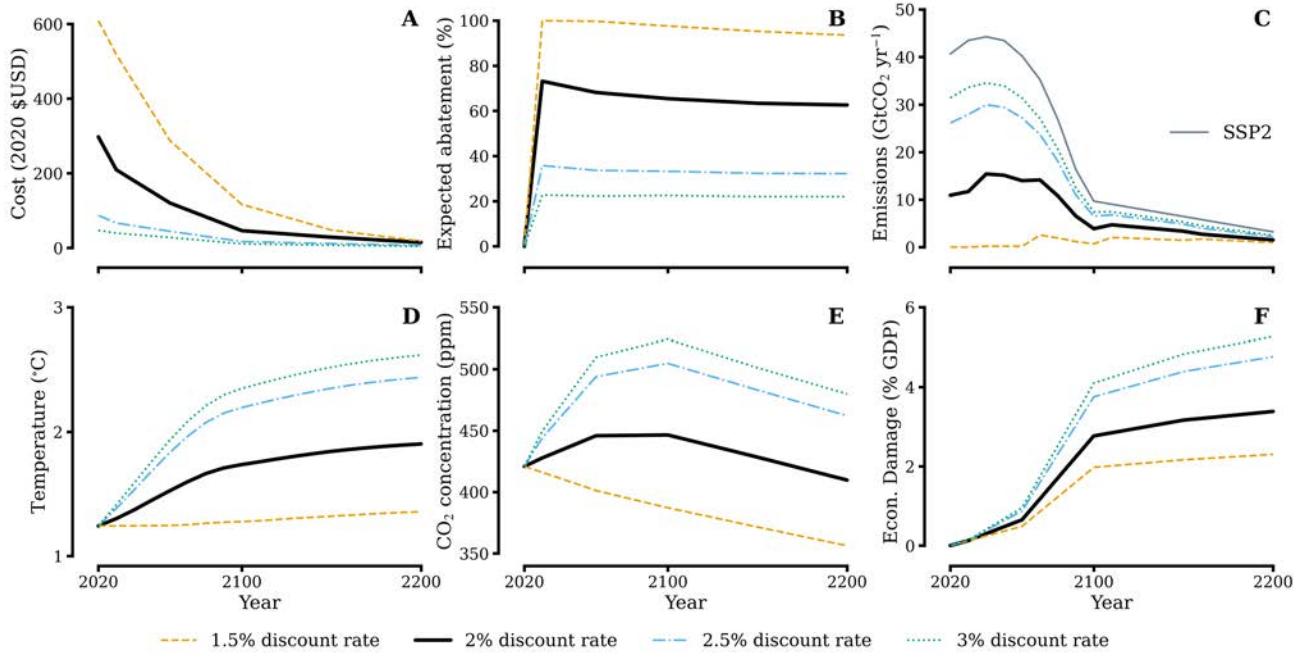


Figure 6: CAP6 output for four discount rates using the “no free lunches” cost curve calibration.

465 maintaining less than 2 °C warming. This shows that even if the cost of abatement is considerably
 466 higher than the IPCC foretells, keeping total warming below 2 °C is still optimal within CAP6 when
 467 a 2% discount rate is used.

468 Running CAP6 with the “no free lunches” calibration and a 2.5% or 3% discount rates show
 469 similar results as the 2% rate, with higher optimal prices, more near-term warming, and higher CO₂
 470 concentrations. In this case, however, we find that using a 2.5% or 3% discount rate exceeds 2 °C
 471 warming in 2100, thus exceeding the upper bound of targeted warming in the Paris agreement. This
 472 shows that if abatement turns out to be more costly than we expect, using a higher discount rate in
 473 climate policy makes the world’s ability of achieving the warming targets in the Paris agreement far
 474 more tenuous.

475 The only exception to the pattern above – the “no free lunches” MACC leading to less abatement
 476 and more warming – is the 1.5% discount rate policy, which still abates nearly 100% of emissions in the
 477 near term. This can be explained by this agent having both a low discount rate and low risk tolerance,
 478 and therefore sacrifices considerable consumption to minimize both experienced and potential future
 479 damages owing to climate change.

480 5.3 Ensemble model analysis

481 We probe the influence of uncertainty in exogenous model parameters on CO₂ price paths, temperature
 482 change, CO₂ concentrations, and economic damages incurred in our ensemble runs, shown in Figure 7.
 483 We find that CO₂ price paths decline over time, regardless of socio-economic specification, owing to
 484 agent risk response and technological progress. The level of CO₂ price varies between baselines because
 485 the MACC is baseline dependent (see Eqn. (2.12)); for the same fraction of emissions abated, agents
 486 pay different prices depending on the baseline. Finally, cost variance is highly stratified across baselines,

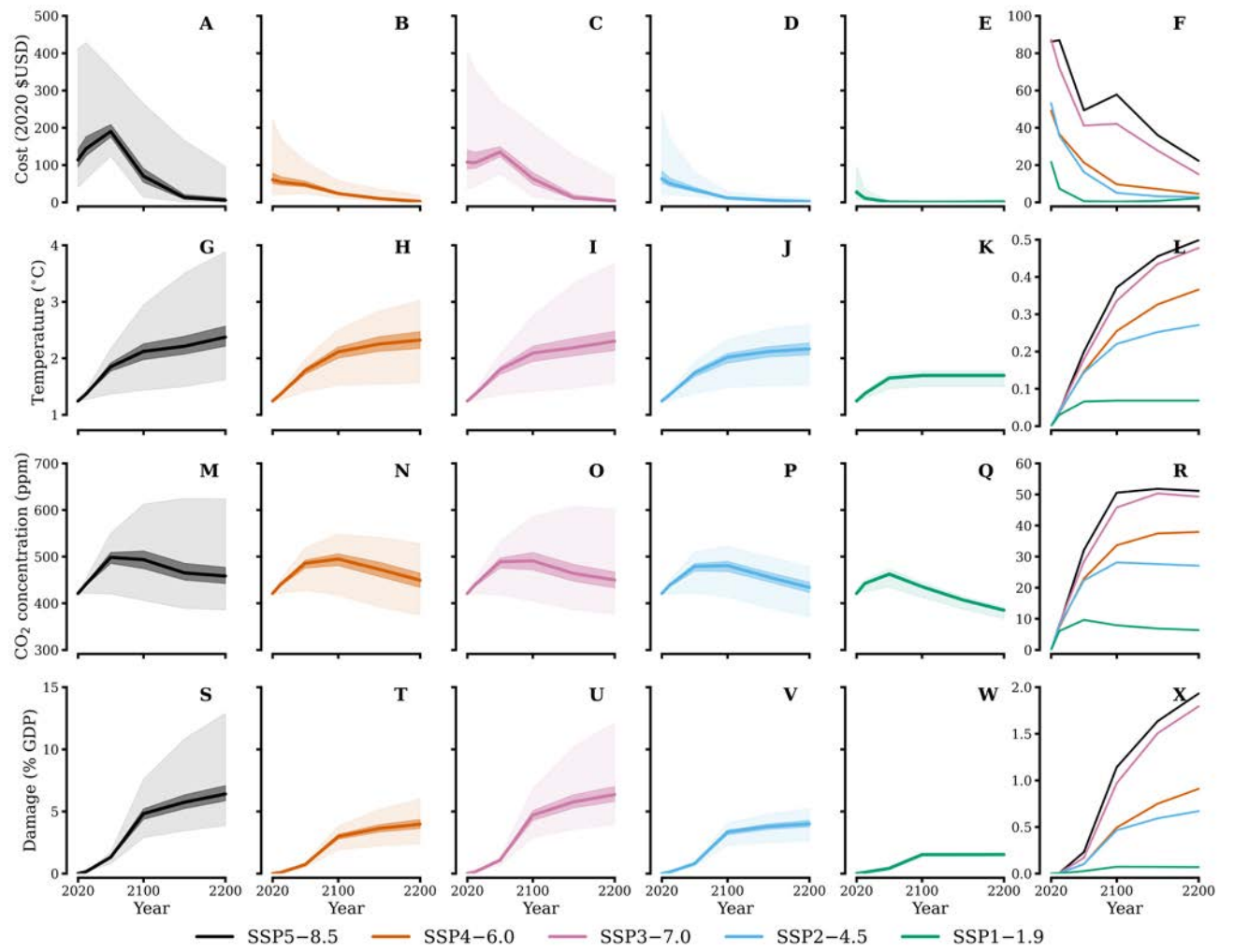


Figure 7: Cost (top row, panels A–E), temperature (second from top, panels G–K), CO₂ concentrations (third from top, panels M–Q), and economic damages (bottom row, panels S–W) from our ensemble model runs. Dark (light, resp.) shaded region represents the 36th–64th (1st–99th, resp.) percentile range, solid lines represent the median time series. In the final column (panels F, L, R, and X) we plot the standard deviation of each parameter distribution in time.

487 see panel 7F.

488 Central estimates of temperature, CO₂ concentrations, and economic damages,¹⁷ however, do not
489 see significant differences in central estimates across baselines as was observed in CO₂ prices. This
490 owes to suggested policy in CAP6 being consistent across baselines; the only difference is the price of
491 implementing said policy. Hence, the impact variables are relatively insensitive to baseline choice. This
492 is a notable result, as it implies CAP6 finds an optimal outcome across emissions baselines for a given
493 calibration. The variance in each impact variable however, displayed in panels 7L,R,X, is sensitive to the
494 choice in baseline, with high (low, resp.) emissions scenarios having the highest (lowest, resp.) amount
495 of variance. This can be explained by considering the consequences of inaction (i.e., high discount rate
496 policies). In a high emissions scenario such as SSP5–8.5, inaction leads to more emissions, and thus
497 higher impacts than in a low emissions scenario such as SSP2–4.5. Hence, the variance in each impact
498 variable are all higher for high emissions scenarios than in low emissions scenarios.

499 **5.3.1 Variance decomposition of ensemble results**

500 The significant stratification of uncertainty in our output variables shown in Figure 7 motivates further
501 study; is it high discount rates that control prices, for example, or rates of technological change? To
502 this end, we perform a regression analysis of CO₂ price and the impact variables studied above at every
503 point in time against parameter values, and plot the fraction of total r^2 attributable to each parameter
504 in Figure 8 (see Online Appendix I for details and supporting figures).

505 For prices, we find that the discount rate (i.e., EIS and PRTP) dominate uncertainty in the near term
506 (i.e., prior to 2100). This owes to these parameters dictating individual attitudes towards time-related
507 risk and discounting. In early periods of the model, climate damages are highly uncertain. Therefore,
508 any abatement action that is taken is with the intent to rule out the most catastrophic outcomes and
509 secure future welfare; the extent to which individuals respond to this threat of catastrophe is governed
510 by the discount rate, thus determining the level of early mitigation action and driving costs. On longer
511 timescales (past 2100), climate damages have been more distinctly realized, and the number of possible
512 futures have narrowed. Individuals must come to grips with their damaged future, and generally begin
513 investing more stringently in emissions abatement. This comes at a cost, a cost that is determined
514 by how much cheaper abatement technologies have become in the time it took to reach this decision.
515 In particular, high prices in late periods are almost entirely attributable to low rates of technological
516 change across SSPs.

517 For the impact variables, however, a different story emerges: the influence of the discount rate is
518 pronounced for much longer than in the case of CO₂ prices. This owes to inactivity early on leading to
519 long-term consequences in the form of climate-economic impacts that cannot simply be fixed by more
520 spending on abatement.¹⁸ Indeed, while technological change can certainly halt any further increase in
521 global mean surface temperature, for example, it cannot undo past malfeasance.¹⁹ Hence, the discount

¹⁷We refer to this set of variables as “impact variables” for the remainder of this discussion.

¹⁸This conclusion relies on a high cost of net-negative emissions; if a breakthrough in direct air capture (DAC) technologies occurs, then we would expect the variance explained in impact variables owing to technological growth to be higher, as net-negative emissions would enable long-run temperatures, CO₂ concentrations, and economic losses to be changed, perhaps significantly so, depending on how expensive DAC turns out to be.

¹⁹An important qualification to this conclusion is that we do not consider solar geoengineering, which could lead to

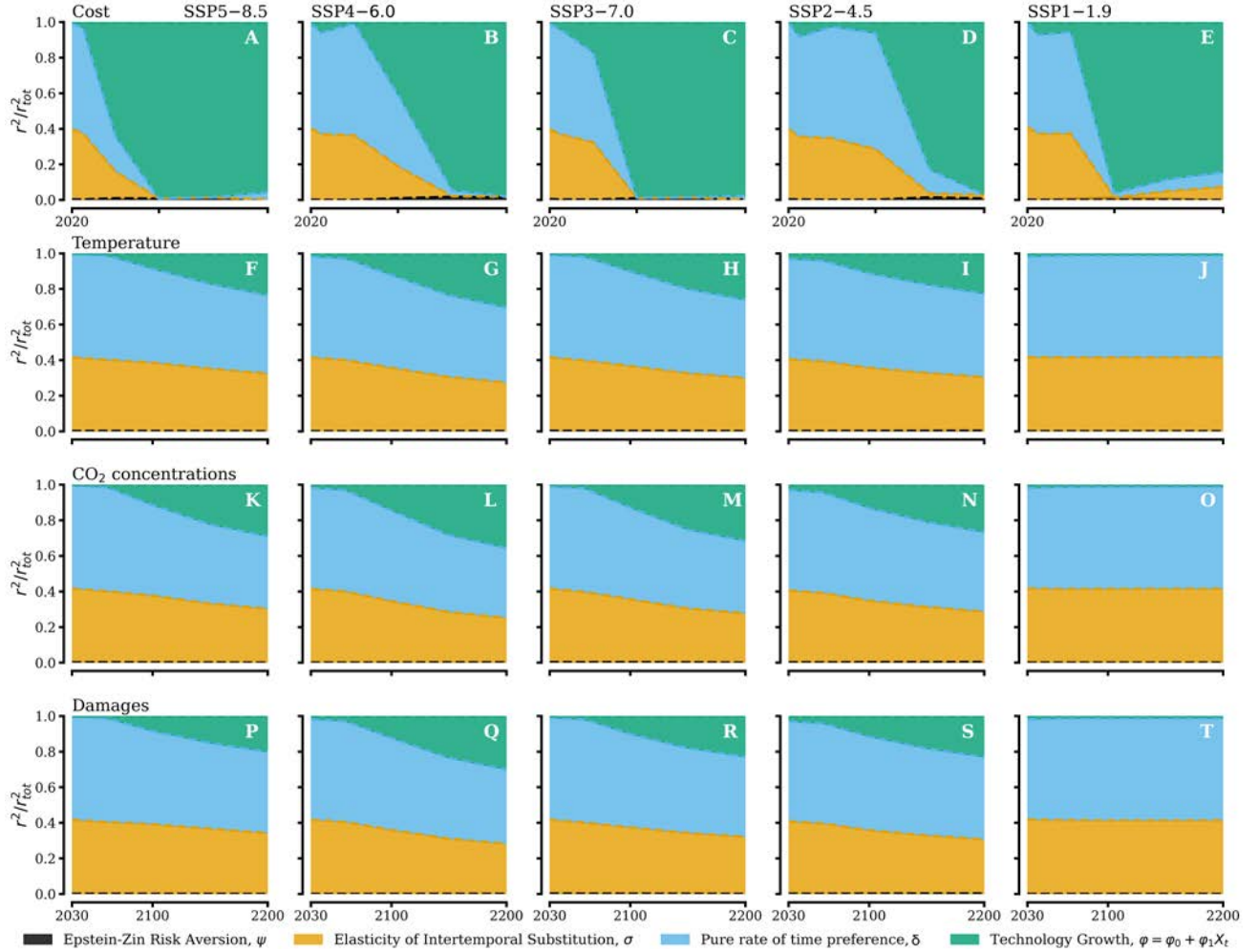


Figure 8: Fraction of total variance (calculated as total r^2) attributable to each model parameter for carbon prices (top row, panels A–E), temperature (second row, panels F–J), CO₂ concentrations (third row, panels K–O), and economic damages (bottom row, panels P–T). Each column represents a different SSP.

Note: Cost variance (top row) begins in 2020 whereas temperature, CO₂ concentrations, and economic damages (bottom three rows) begin in 2030, as the model is initialized with the same climate conditions and no damages incurred, leading to zero variance in 2020 for the latter three variables.

522 rate has a much more pronounced influence on far-distant temperature rise, atmospheric CO₂ levels,
523 and economic damages than in the case of CO₂ prices.

524 Interestingly, Figure 8 shows that the influence of RA (i.e., the value of ψ) is suppressed for CAP6
525 output uncertainty²⁰ relative to other model inputs. We postulate that this owes to the risk aversion
526 captured by ψ (i.e., the Epstein-Weil-Zin sense of risk aversion across states of nature) is relatively less
527 important to risk across states of time. Given the large residence time of CO₂ in the atmosphere, it
528 stands to reason that the impact of risk aversion with respect to time would dwarf the impact of risk
529 aversion across states of nature. Indeed, the results of Figure 8 provide resounding support for this
530 theory: risk aversion across states of time (captured by EIS) drowns out the influence of risk across
531 states of nature (as captured by RA).

532 6 Conclusion

533 Over a decade ago, Lord Nicholas Stern wrote that “Presenting the [climate] problem as risk-management
534 is likely to point strongly towards a policy for a rapid transition to a low-carbon economy” (Stern,
535 2013).²¹ Our framework takes this view seriously, and, in the final analysis, shows the wisdom in
536 Stern’s words. By treating CO₂ as a risky asset and calculating the optimal CO₂ price and associated
537 abatement policy using U.S. EPA-consistent discount rates, we find that optimal policy limits warming
538 below 2 °C in 2100 for each discount rate we considered. Practically speaking, this corresponds to
539 cutting > 70% of CO₂ emissions in relatively short order; a “rapid transition to a low-carbon econ-
540 omy” indeed. Our results flip the conventional view of climate policy on its head; rather than abating
541 progressively more CO₂ emissions as time goes on (and damages are felt more acutely), our model
542 suggests stringent early abatement as a ‘hedge’ against potentially severe damages associated with
543 climate change.

544 Evidently our framework for computing optimal climate policies is idealized, and in practice, a
545 number of additional considerations are necessary for formulating robust climate policy. For example,
546 we compute a globally “optimal carbon tax” as a proxy for the overall strength of climate policy, not
547 as an actual policy guide.²² Prospects for such a common global carbon tax are bleak, to put it mildly.
548 Therefore, useful extensions of this work would analyze the transition risk towards zero emissions
549 policies, i.e., by considering asset stranding and adjustment costs (Campiglio et al., 2022), the potential
550 for a ‘run on fossil fuels’ induced by an expected transition away from fossil fuel use (Barnett, 2023),
551 or considering the distributional effects of heterogeneous climate policy mixes in different nations (as
552 explored in Clausing and Wolfram, 2023). More work in this direction could prove both scientifically
553 and economically insightful as well as immediately applicable in a wide variety of policy settings.

increased spending influencing temperature, CO₂ concentration, and economic damages levels in both the short- and long-term.

²⁰This is not to say that RA has no impact on price levels, as increasing (decreasing, resp.) RA does slightly raise (lower, resp.) near term prices, see Online Appendix J.

²¹Others, like Nordhaus (2007), criticized Stern at the time, while Weitzman (2007) argued that Stern was “right for the wrong reasons”, reasons subsequently developed in Weitzman (2009, 2012).

²²Another limitation is that we compute the optimal carbon tax with a single exogenous discount rate. In reality, the discount rate will respond to the level of risk (Lucas, 1976) and is uncertain on long time horizons (Weitzman, 1998). Allowing for a dynamic discount rate in our framework is a potentially fruitful avenue of future work.

554 **Author ORCIDs**

- 555 • Adam Michael Bauer: 0000-0002-7471-8934
556 • Cristian Proistosescu: 0000-0002-1717-124X
557 • Gernot Wagner: 0000-0001-6059-0688

558 **Acknowledgements**

559 The authors thank Simon Dietz, Romain Fillon, Bob Kopp, Geoffrey Heal, Glenn Hubbard, Bob Lit-
560 terman, Bruce McCarl, James Rising, Chris Smith, Thomas Stoerk, Andrew Wilson, three anonymous
561 reviewers, and seminar audiences at Columbia University, the Center for Social and Environmental Fu-
562 tures at the University of Colorado Boulder, the 2022 fall meeting of the American Geophysical Union,
563 and the 2023 summer conferences of the Association of Environmental and Resource Economists and
564 the European Association of Environmental and Resource Economists for providing useful feedback on
565 this work. The authors thank Alaa Al Khourdajie for providing the data from AR6 WGIII's cost of
566 mitigation figure, W. Matthew Alampay Davis and Steve Rose for helpful discussions of climate dam-
567 age functions, David C. Lafferty for his contributions to Figure 3, and Jaydeep Pillai for testing the
568 public release version of the code. AMB thanks Columbia Business School for their hospitality while
569 this work was being completed, and acknowledges support from the Gies College of Business Office of
570 Risk Management and Insurance at the University of Illinois Urbana-Champaign, Columbia Business
571 School, and a National Science Foundation Graduate Research Fellowship grant No. DGE 21-46756.
572 CP was supported by the Gies College of Business Office of Risk Management and Insurance Research
573 at the University of Illinois Urbana-Champaign. Computations were performed on the Keeling com-
574 puting cluster, a computing resource operated by the School of Earth, Society and the Environment
575 (SESE) at the University of Illinois Urbana-Champaign.

576 **Disclosure statements**

577 *Adam Michael Bauer*

578 At the time of submission, I hold a short-term consultancy position at the World Bank's Climate Change
579 Group; the work being completed under this consultancy is unrelated to this publication (hence why
580 I do not declare an affiliation to the World Bank Group in the above). I have no other conflicts of
581 interest to disclose.

582 *Cristian Proistosescu*

583 I have no conflicts of interest to disclose.

584 *Gernot Wagner*

585 I am on the corporate advisory board of CarbonPlan. I have no other conflicts of interest to disclose.

586 **Author contributions**

587 Cristian Proistosescu and Gernot Wagner conceived of the study. Adam Michael Bauer wrote the code,
588 designed numerical experiments, performed literature review, and made the figures. The first draft of
589 the paper was written by Adam Michael Bauer, and all authors assisted in editing this draft to shape
590 the final submitted manuscript. All authors have approved the submitted verison.

591 **Data Availability**

592 The code for the Carbon Asset Pricing model – AR6 (CAP6) can be found at the following Github
593 repository: github.com/adam-bauer-34/cap6.

594 **References**

- 595 D. Acemoglu, P. Aghion, L. Bursztyn, and D. Hemous. The Environment and Directed Technical
596 Change. *American Economic Review*, 102(1):131–166, Feb. 2012. ISSN 0002-8282. doi: 10.1257/aer.
597 102.1.131. URL <https://pubs.aeaweb.org/doi/10.1257/aer.102.1.131>.
- 598 M. R. Allen, D. J. Frame, C. Huntingford, C. D. Jones, J. A. Lowe, M. Meinshausen, and N. Mein-
599 shausen. Warming caused by cumulative carbon emissions towards the trillionth tonne. *Nature*,
600 458(7242):1163–1166, Apr. 2009. ISSN 0028-0836, 1476-4687. doi: 10.1038/nature08019. URL
601 <http://www.nature.com/articles/nature08019>.
- 602 D. I. Armstrong McKay, A. Staal, J. F. Abrams, R. Winkelmann, B. Sakschewski, S. Loriani, I. Fetzer,
603 S. E. Cornell, J. Rockström, and T. M. Lenton. Exceeding 1.5°C global warming could trigger multiple
604 climate tipping points. *Science*, 377(6611):eabn7950, Sept. 2022. ISSN 0036-8075, 1095-9203. doi:
605 10.1126/science.abn7950. URL <https://www.science.org/doi/10.1126/science.abn7950>.
- 606 M. Barnett. A Run on Oil? Climate Policy and Stranded Assets Risk. Working Paper, 2023. URL
607 <https://www.ssrn.com/abstract=4346525>.
- 608 M. Barnett, W. Brock, and L. P. Hansen. Pricing Uncertainty Induced by Climate Change. *The
609 Review of Financial Studies*, 33(3):1024–1066, Mar. 2020. ISSN 0893-9454, 1465-7368. doi: 10.1093/
610 rfs/hhz144. URL <https://academic.oup.com/rfs/article/33/3/1024/5735312>.
- 611 L. Barrage and W. Nordhaus. Policies, Projections, and the Social Cost of Carbon: Results from the
612 DICE-2023 Model. Technical Report w31112, National Bureau of Economic Research, Cambridge,
613 MA, Apr. 2023. URL <http://www.nber.org/papers/w31112.pdf>.
- 614 M. D. Bauer and G. D. Rudebusch. The Rising Cost of Climate Change: Evidence from the Bond Mar-
615 ket. *Federal Reserve Bank of San Francisco, Working Paper Series*, pages 1.000–39.000, July 2020.
616 doi: 10.24148/wp2020-25. URL <https://www.frbsf.org/economic-research/publications/working-papers/2020/25/>.

- 618 L. Bretschger and A. Vinogradova. Growth and Mitigation Policies with Uncertain Climate Damage.
619 Working Paper 5085, CESifo, Munich, 2014. URL <https://www.cesifo.org/en/publications/2014/working-paper/growth-and-mitigation-policies-uncertain-climate-damage>.
- 621 M. Burke, W. M. Davis, and N. S. Diffenbaugh. Large potential reduction in economic damages under
622 UN mitigation targets. *Nature*, 557(7706):549–553, May 2018. ISSN 0028-0836, 1476-4687. doi:
623 10.1038/s41586-018-0071-9. URL <http://www.nature.com/articles/s41586-018-0071-9>.
- 624 Y. Cai and T. S. Lontzek. The Social Cost of Carbon with Economic and Climate Risks. *Journal of
625 Political Economy*, 127(6):2684–2734, Dec. 2019. ISSN 0022-3808, 1537-534X. doi: 10.1086/701890.
626 URL <https://www.journals.uchicago.edu/doi/10.1086/701890>.
- 627 Y. Cai, T. M. Lenton, and T. S. Lontzek. Risk of multiple interacting tipping points should encourage
628 rapid CO₂ emission reduction. *Nature Climate Change*, 6(5):520–525, May 2016. ISSN 1758-678X,
629 1758-6798. doi: 10.1038/nclimate2964. URL <http://www.nature.com/articles/nclimate2964>.
- 630 E. Campiglio, S. Dietz, and F. Venmans. Optimal Climate Policy as If the Transition Matters. Working
631 Paper 10139, CESifo, Munich, 2022. URL <https://www.cesifo.org/en/publications/2022/working-paper/optimal-climate-policy-if-transition-matters>.
- 633 K. A. Clausing and C. Wolfram. Carbon Border Adjustments, Climate Clubs, and Subsidy Races When
634 Climate Policies Vary. *Journal of Economic Perspectives*, 37(3):137–162, Sept. 2023. ISSN 0895-3309.
635 doi: 10.1257/jep.37.3.137. URL <https://www.aeaweb.org/articles?id=10.1257/jep.37.3.137>.
- 636 T. F. Coleman, N. S. Dumont, W. Li, W. Liu, and A. Rubtsov. Optimal Pricing of Climate Risk.
637 *Computational Economics*, Aug. 2021. ISSN 0927-7099, 1572-9974. doi: 10.1007/s10614-021-10179-6.
638 URL <https://link.springer.com/10.1007/s10614-021-10179-6>.
- 639 Committee on Assessing Approaches to Updating the Social Cost of Carbon, Board on Environmental
640 Change and Society, Division of Behavioral and Social Sciences and Education, and National
641 Academies of Sciences, Engineering, and Medicine. *Valuing Climate Changes: Updating Estimation
642 of the Social Cost of Carbon Dioxide*. National Academies Press, Washington, D.C., 2017. ISBN
643 9780309454209. doi: 10.17226/24651. URL <https://www.nap.edu/catalog/24651>.
- 644 Council of Economic Advisors. Discounting for public policy: Theory and recent ev-
645 idence on the merits of updating the discount rate. Technical report, Washington,
646 DC, 2017. URL https://obamawhitehouse.archives.gov/sites/default/files/page/files/201701_cea_discounting_issue_brief.pdf.
- 648 J. C. Cox, S. A. Ross, and M. Rubinstein. Option pricing: A simplified approach. *Journal of Financial
649 Economics*, 7(3):229–263, Sept. 1979. ISSN 0304405X. doi: 10.1016/0304-405X(79)90015-1. URL
650 <https://linkinghub.elsevier.com/retrieve/pii/0304405X79900151>.
- 651 H. Damon Matthews, K. B. Tokarska, J. Rogelj, C. J. Smith, A. H. MacDougall, K. Haustein,
652 N. Mengis, S. Sippel, P. M. Forster, and R. Knutti. An integrated approach to quantifying uncer-
653 tainties in the remaining carbon budget. *Communications Earth & Environment*, 2(1):7, Jan. 2021.

- 654 ISSN 2662-4435. doi: 10.1038/s43247-020-00064-9. URL <https://www.nature.com/articles/s43247-020-00064-9>.
- 655
- 656 K. Daniel, R. Litterman, and G. Wagner. Applying Asset Pricing Theory to Calibrate the Price of
657 Climate Risk. Technical Report w22795, National Bureau of Economic Research, Cambridge, MA,
658 Nov. 2016. URL <http://www.nber.org/papers/w22795.pdf>.
- 659 K. D. Daniel, R. B. Litterman, and G. Wagner. Declining CO₂ price paths. *Proceedings of the*
660 *National Academy of Sciences*, 116(42):20886–20891, Oct. 2019. ISSN 0027-8424, 1091-6490. doi:
661 10.1073/pnas.1817444116. URL <http://www.pnas.org/lookup/doi/10.1073/pnas.1817444116>.
- 662 S. Dietz and F. Venmans. Cumulative carbon emissions and economic policy: In search of general
663 principles. *Journal of Environmental Economics and Management*, 96:108–129, July 2019. ISSN
664 00950696. doi: 10.1016/j.jeem.2019.04.003. URL <https://linkinghub.elsevier.com/retrieve/pii/S0095069618302122>.
- 665
- 666 S. Dietz, J. Rising, T. Stoerk, and G. Wagner. Economic impacts of tipping points in the climate
667 system. *Proceedings of the National Academy of Sciences*, 118(34):e2103081118, Aug. 2021. ISSN
668 0027-8424, 1091-6490. doi: 10.1073/pnas.2103081118. URL <https://pnas.org/doi/full/10.1073/pnas.2103081118>.
- 669
- 670 M. A. Drupp, M. C. Freeman, B. Groom, and F. Nesje. Discounting Disentangled. *American Economic*
671 *Journal: Economic Policy*, 10(4):109–134, Nov. 2018. ISSN 1945-7731, 1945-774X. doi: 10.1257/
672 pol.20160240. URL <https://pubs.aeaweb.org/doi/10.1257/pol.20160240>.
- 673
- 674 M. T. Dvorak, K. C. Armour, D. M. W. Frierson, C. Proistosescu, M. B. Baker, and C. J. Smith. Esti-
675 mating the timing of geophysical commitment to 1.5 and 2.0 °C of global warming. *Nature Climate*
676 *Change*, 12(6):547–552, June 2022. ISSN 1758-678X, 1758-6798. doi: 10.1038/s41558-022-01372-y.
677 URL <https://www.nature.com/articles/s41558-022-01372-y>.
- 678
- 679 L. G. Epstein and S. E. Zin. Substitution, Risk Aversion, and the Temporal Behavior of Consumption
and Asset Returns: A Theoretical Framework. *Econometrica*, 57(4):937, July 1989. ISSN 00129682.
doi: 10.2307/1913778. URL <https://www.jstor.org/stable/1913778?origin=crossref>.
- 680
- 681 L. G. Epstein and S. E. Zin. Substitution, Risk Aversion, and the Temporal Behavior of Consumption
and Asset Returns: An Empirical Analysis. *Journal of Political Economy*, 99(2):263–286, Apr. 1991.
682 ISSN 0022-3808, 1537-534X. doi: 10.1086/261750. URL <https://www.journals.uchicago.edu/doi/10.1086/261750>.
- 683
- 684 O. Geoffroy, D. Saint-Martin, G. Bellon, A. Volodire, D. J. L. Olivié, and S. Tytéca. Transient climate
685 response in a two-layer energy-balance model. part ii: Representation of the efficacy of deep-ocean
686 heat uptake and validation for cmip5 aogcms. *Journal of Climate*, 26(6):1859–1876, 2013a. ISSN
687 08948755, 15200442. URL <http://www.jstor.org/stable/26192253>.
- 688
- 689 O. Geoffroy, D. Saint-Martin, D. Olivié, A. Volodire, G. Bellon, and S. Tytéca. Transient cli-
mate response in a two-layer energy-balance model. part i: Analytical solution and parameter

- 690 calibration using cmip5 aogcm experiments. *Journal of Climate*, 26:1841–1857, 03 2013b. doi:
691 10.1175/JCLI-D-12-00195.1.
- 692 K. Gillingham and J. H. Stock. The Cost of Reducing Greenhouse Gas Emissions. *Journal of Economic
693 Perspectives*, 32(4):53–72, Nov. 2018. ISSN 0895-3309. doi: 10.1257/jep.32.4.53. URL <https://pubs.aeaweb.org/doi/10.1257/jep.32.4.53>.
- 695 M. Golosov, J. Hassler, P. Krusell, and A. Tsyvinski. Optimal Taxes on Fossil Fuel in General
696 Equilibrium. *Econometrica*, 82(1):41–88, 2014. ISSN 0012-9682. doi: 10.3982/ECTA10217. URL
697 <http://doi.wiley.com/10.3982/ECTA10217>.
- 698 M. C. Hänsel, M. A. Drupp, D. J. Johansson, F. Nesje, C. Azar, M. C. Freeman, B. Groom, and
699 T. Sterner. Climate economics support for the UN climate targets. *Nature Climate Change*, 10(8):
700 781–789, 2020.
- 701 Z. Hausfather and G. P. Peters. Emissions – the ‘business as usual’ story is misleading. *Nature*,
702 577(7792):618–620, Jan. 2020. doi: 10.1038/d41586-020-00177-3. URL <https://www.nature.com/articles/d41586-020-00177-3>.
- 704 E. Hawkins and R. Sutton. The Potential to Narrow Uncertainty in Regional Climate Predictions.
705 *Bulletin of the American Meteorological Society*, 90(8):1095–1108, Aug. 2009. ISSN 0003-0007,
706 1520-0477. doi: 10.1175/2009BAMS2607.1. URL <https://journals.ametsoc.org/doi/10.1175/2009BAMS2607.1>.
- 708 P. H. Howard and T. Sterner. Few and Not So Far Between: A Meta-analysis of Climate Dam-
709 age Estimates. *Environmental and Resource Economics*, 68(1):197–225, Sept. 2017. ISSN 0924-
710 6460, 1573-1502. doi: 10.1007/s10640-017-0166-z. URL <http://link.springer.com/10.1007/s10640-017-0166-z>.
- 712 Intergovernmental Panel on Climate Change. Climate change 2021: The physical science basis. 2021.
713 URL https://report.ipcc.ch/ar6wg1/pdf/IPCC_AR6_WGI_FinalDraft_FullReport.pdf.
- 714 Intergovernmental Panel on Climate Change. Climate change 2022: Impacts, adaptation, and
715 vulnerability. 2022a. URL https://report.ipcc.ch/ar6wg2/pdf/IPCC_AR6_WGII_FinalDraft_FullReport.pdf.
- 717 Intergovernmental Panel on Climate Change. Climate change 2022: Mitigation of climate change.
718 2022b. URL https://report.ipcc.ch/ar6wg3/pdf/IPCC_AR6_WGIII_FinalDraft_FullReport.pdf.
- 720 International Energy Agency. Direct Air Capture 2022 – Analysis. Technical report, International
721 Energy Agency, Apr. 2022. URL <https://www.iea.org/reports/direct-air-capture-2022>.
- 722 A. B. Jaffe and R. N. Stavins. The energy paradox and the diffusion of conservation technology. *Re-
723 source and Energy Economics*, 16(2):91–122, May 1994. ISSN 09287655. doi: 10.1016/0928-7655(94)
724 90001-9. URL <https://linkinghub.elsevier.com/retrieve/pii/0928765594900019>.

- 725 K. Johnson, D. Martin, X. Zhang, C. DeYoung, and A. Stolberg. Carbon Dioxide Removal Options: A
726 Literature Review Identifying Carbon Removal Potentials and Costs. 2017. URL <http://deepblue.lib.umich.edu/handle/2027.42/136610>.
- 728 F. Joos, R. Roth, J. S. Fuglestvedt, G. P. Peters, I. G. Enting, W. von Bloh, V. Brovkin, E. J.
729 Burke, M. Eby, N. R. Edwards, T. Friedrich, T. L. Frölicher, P. R. Halloran, P. B. Holden,
730 C. Jones, T. Kleinen, F. T. Mackenzie, K. Matsumoto, M. Meinshausen, G.-K. Plattner, A. Reisinger,
731 J. Segschneider, G. Shaffer, M. Steinacher, K. Strassmann, K. Tanaka, A. Timmermann, and A. J.
732 Weaver. Carbon dioxide and climate impulse response functions for the computation of green-
733 house gas metrics: a multi-model analysis. *Atmospheric Chemistry and Physics*, 13(5):2793–2825,
734 Mar. 2013. ISSN 1680-7324. doi: 10.5194/acp-13-2793-2013. URL <https://acp.copernicus.org/articles/13/2793/2013/>.
- 736 R. E. Kopp, R. L. Shwom, G. Wagner, and J. Yuan. Tipping elements and climate–economic shocks:
737 Pathways toward integrated assessment. *Earth’s Future*, 4(8):346–372, 2016.
- 738 M. J. Kotchen, J. A. Rising, and G. Wagner. The costs of “costless” climate mitigation. *Science*,
739 382(6674):1001–1003, Dec. 2023. ISSN 0036-8075, 1095-9203. doi: 10.1126/science.adj2453. URL
740 <https://www.science.org/doi/10.1126/science.adj2453>.
- 741 A. Lans Bovenberg and S. Smulders. Environmental quality and pollution-augmenting technological
742 change in a two-sector endogenous growth model. *Journal of Public Economics*, 57(3):369–391, July
743 1995. ISSN 00472727. doi: 10.1016/0047-2727(95)80002-Q. URL <https://linkinghub.elsevier.com/retrieve/pii/004727279580002Q>.
- 745 F. Lehner, C. Deser, N. Maher, J. Marotzke, E. M. Fischer, L. Brunner, R. Knutti, and E. Hawkins.
746 Partitioning climate projection uncertainty with multiple large ensembles and CMIP5/6. *Earth
747 System Dynamics*, 11(2):491–508, May 2020. ISSN 2190-4987. doi: 10.5194/esd-11-491-2020. URL
748 <https://esd.copernicus.org/articles/11/491/2020/>.
- 749 D. Lemoine. The Climate Risk Premium: How Uncertainty Affects the Social Cost of Carbon. *Journal
750 of the Association of Environmental and Resource Economists*, 8(1):27–57, Jan. 2021. ISSN 2333-
751 5955, 2333-5963. doi: 10.1086/710667. URL <https://www.journals.uchicago.edu/doi/10.1086/710667>.
- 753 D. Lemoine and I. Rudik. Managing Climate Change Under Uncertainty: Recursive Integrated
754 Assessment at an Inflection Point. *Annual Review of Resource Economics*, 9(1):117–142, Oct.
755 2017. ISSN 1941-1340, 1941-1359. doi: 10.1146/annurev-resource-100516-053516. URL <https://www.annualreviews.org/doi/10.1146/annurev-resource-100516-053516>.
- 757 D. Lemoine and C. P. Traeger. Ambiguous tipping points. *Journal of Economic Behavior &
758 Organization*, 132:5–18, Dec. 2016a. ISSN 01672681. doi: 10.1016/j.jebo.2016.03.009. URL
759 <https://linkinghub.elsevier.com/retrieve/pii/S0167268116300221>.
- 760 D. Lemoine and C. P. Traeger. Economics of tipping the climate dominoes. *Nature Climate Change*,
761 6(5):514–519, May 2016b. ISSN 1758-678X, 1758-6798. doi: 10.1038/nclimate2902. URL <https://www.nature.com/articles/nclimate2902>.

- 763 T. M. Lenton, H. Held, E. Kriegler, J. W. Hall, W. Lucht, S. Rahmstorf, and H. J. Schellnhuber.
764 Tipping elements in the Earth’s climate system. *Proceedings of the National Academy of Sciences*,
765 105(6):1786–1793, Feb. 2008. ISSN 0027-8424, 1091-6490. doi: 10.1073/pnas.0705414105. URL
766 <https://pnas.org/doi/full/10.1073/pnas.0705414105>.
- 767 R. E. Lucas. Econometric policy evaluation: A critique. *Carnegie-Rochester Conference Series on*
768 *Public Policy*, 1:19–46, Jan. 1976. ISSN 01672231. doi: 10.1016/S0167-2231(76)80003-6. URL
769 <https://linkinghub.elsevier.com/retrieve/pii/S0167223176800036>.
- 770 McKinsey & Company. *Pathways to a low-carbon economy: Version 2 of the global greenhouse gas*
771 *abatement cost curve*. McKinsey & Company, Stockholm, Sept. 2013. URL <https://www.mckinsey.com/capabilities/sustainability/our-insights/pathways-to-a-low-carbon-economy>.
- 773 M. Meinshausen, Z. R. J. Nicholls, J. Lewis, M. J. Gidden, E. Vogel, M. Freund, U. Beyerle,
774 C. Gessner, A. Nauels, N. Bauer, J. G. Canadell, J. S. Daniel, A. John, P. B. Krummel, G. Lud-
775 erer, N. Meinshausen, S. A. Montzka, P. J. Rayner, S. Reimann, S. J. Smith, M. van den Berg,
776 G. J. M. Velders, M. K. Vollmer, and R. H. J. Wang. The shared socio-economic pathway
777 (SSP) greenhouse gas concentrations and their extensions to 2500. *Geoscientific Model Devel-*
778 *opment*, 13(8):3571–3605, Aug. 2020. ISSN 1991-9603. doi: 10.5194/gmd-13-3571-2020. URL
779 <https://gmd.copernicus.org/articles/13/3571/2020/>.
- 780 National Center for Energy Economics. *Supplementary Material for the Regulatory Impact Analysis*
781 *for the Supplemental Proposed Rulemaking, “Standards of Performance for New, Reconstructed, and*
782 *Modified Sources and Emissions Guidelines for Existing Sources: Oil and Natural Gas Sector Climate*
783 *Review”*. U.S. Environmental Protection Agency, Washington D.C., Sept. 2022.
- 784 National Research Council. *Climate Intervention: Carbon Dioxide Removal and Reliable Sequestration*.
785 National Academies Press, Washington, D.C., June 2015. ISBN 9780309305297. doi: 10.17226/18805.
786 URL <http://www.nap.edu/catalog/18805>.
- 787 New York State Energy Research and Development Authority and Resources for the Future. Estimating
788 the cost of carbon: two approaches. Technical report, Oct. 2020. URL https://media.rff.org/documents/RFF_NYSERDA_Valuing_Carbon_Synthesis_Memo.pdf.
- 790 R. G. Newell, W. A. Pizer, and B. C. Prest. A Discounting Rule for the Social Cost of Carbon. *Journal*
791 *of the Association of Environmental and Resource Economists*, 9(5):1017–1046, Sept. 2022. ISSN
792 2333-5955, 2333-5963. doi: 10.1086/718145. URL <https://www.journals.uchicago.edu/doi/10.1086/718145>.
- 794 J. Nielsen-Gammon and M. Behl. Improving the value of climate data and models for assessing climate
795 impacts and policies. Technical report, University Corporation for Atmospheric Research (UCAR),
796 2021. URL <https://opensky.ucar.edu/islandora/object/usclivar:131>.
- 797 W. D. Nordhaus. An Optimal Transition Path for Controlling Greenhouse Gases. *Science*, 258(5086):
798 1315–1319, Nov. 1992. ISSN 0036-8075, 1095-9203. doi: 10.1126/science.258.5086.1315. URL <https://www.sciencemag.org/lookup/doi/10.1126/science.258.5086.1315>.

- 800 W. D. Nordhaus. A review of the stern review on the economics of climate change. *Journal of economic*
801 *literature*, 45(3):686–702, 2007.
- 802 W. D. Nordhaus. Revisiting the social cost of carbon. *Proceedings of the National Academy of Sciences*,
803 114(7):1518–1523, Feb. 2017. ISSN 0027-8424, 1091-6490. doi: 10.1073/pnas.1609244114. URL
804 <https://pnas.org/doi/full/10.1073/pnas.1609244114>.
- 805 R. S. Pindyck. Climate Change Policy: What Do the Models Tell Us? *Journal of Economic Literature*,
806 51(3):860–872, Sept. 2013. ISSN 0022-0515. doi: 10.1257/jel.51.3.860. URL <https://pubs.aeaweb.org/doi/10.1257/jel.51.3.860>.
- 808 K. Rennert, F. Errickson, B. C. Prest, L. Rennels, R. G. Newell, W. Pizer, C. Kingdon, J. Wingenroth,
809 R. Cooke, B. Parthum, D. Smith, K. Cromar, D. Diaz, F. C. Moore, U. K. Müller, R. J. Plevin, A. E.
810 Raftery, H. Ševčíková, H. Sheets, J. H. Stock, T. Tan, M. Watson, T. E. Wong, and D. Anthoff.
811 Comprehensive Evidence Implies a Higher Social Cost of CO₂. *Nature*, Sept. 2022. ISSN 0028-
812 0836, 1476-4687. doi: 10.1038/s41586-022-05224-9. URL <https://www.nature.com/articles/s41586-022-05224-9>.
- 814 K. Riahi, D. P. van Vuuren, E. Kriegler, J. Edmonds, B. C. O'Neill, S. Fujimori, N. Bauer, K. Calvin,
815 R. Dellink, O. Fricko, W. Lutz, A. Popp, J. C. Cuaresma, S. Kc, M. Leimbach, L. Jiang, T. Kram,
816 S. Rao, J. Emmerling, K. Ebi, T. Hasegawa, P. Havlik, F. Humpenöder, L. A. Da Silva, S. Smith,
817 E. Stehfest, V. Bosetti, J. Eom, D. Gernaat, T. Masui, J. Rogelj, J. Strefler, L. Drouet, V. Krey,
818 G. Luderer, M. Harmsen, K. Takahashi, L. Baumstark, J. C. Doelman, M. Kainuma, Z. Klimont,
819 G. Marangoni, H. Lotze-Campen, M. Obersteiner, A. Tabeau, and M. Tavoni. The Shared Socioeconomic
820 Pathways and their energy, land use, and greenhouse gas emissions implications: An overview.
821 *Global Environmental Change*, 42:153–168, Jan. 2017. ISSN 09593780. doi: 10.1016/j.gloenvcha.2016.
822 05.009. URL <https://linkinghub.elsevier.com/retrieve/pii/S0959378016300681>.
- 823 S. K. Rose, D. B. Diaz, and G. J. Blanford. Understanding the Social Cost of Carbon: A Model Di-
824 agnostic and Inter-comparison Study. *Climate Change Economics*, 08(02):1750009, May 2017. ISSN
825 2010-0078, 2010-0086. doi: 10.1142/S2010007817500099. URL <https://www.worldscientific.com/doi/abs/10.1142/S2010007817500099>.
- 827 F. Schroyen and K. O. Aarbu. Attitudes Towards Large Income Risk in Welfare States: An International
828 Comparison, Dec. 2017. URL <https://papers.ssrn.com/abstract=3089690>.
- 829 C. J. Smith, P. M. Forster, M. Allen, N. Leach, R. J. Millar, G. A. Passerello, and L. A. Regayre.
830 FAIR v1.3: a simple emissions-based impulse response and carbon cycle model. *Geoscientific Model
831 Development*, 11(6):2273–2297, June 2018. ISSN 1991-9603. doi: 10.5194/gmd-11-2273-2018. URL
832 <https://gmd.copernicus.org/articles/11/2273/2018/>.
- 833 N. Stern. The Structure of Economic Modeling of the Potential Impacts of Climate Change: Grafting
834 Gross Underestimation of Risk onto Already Narrow Science Models. *Journal of Economic Literature*,
835 51(3):838–859, Sept. 2013. ISSN 0022-0515. doi: 10.1257/jel.51.3.838. URL <https://pubs.aeaweb.org/doi/10.1257/jel.51.3.838>.

- 837 L. Summers and R. Zeckhauser. Policymaking for posterity. *Journal of Risk and Uncertainty*, 37
838 (2-3):115–140, Dec. 2008. ISSN 0895-5646, 1573-0476. doi: 10.1007/s11166-008-9052-y. URL <http://link.springer.com/10.1007/s11166-008-9052-y>.
- 840 United Nations Framework Convention on Climate Change. *Adoption of the Paris Agreement. I: Proposal by the President*. United Nations Office, Geneva, 2015. URL <https://unfccc.int/documents/184656>.
- 843 T. S. Van Den Bremer and F. Van Der Ploeg. The Risk-Adjusted Carbon Price. *American Economic Review*, 111(9):2782–2810, Sept. 2021. ISSN 0002-8282. doi: 10.1257/aer.20180517. URL <https://pubs.aeaweb.org/doi/10.1257/aer.20180517>.
- 846 J. von Neumann and O. Morgenstern. *Theory of games and economic behavior*. Princeton University Press, 1947.
- 848 P. Weil. Nonexpected Utility in Macroeconomics. *The Quarterly Journal of Economics*, 105(1):
849 29, Feb. 1990. ISSN 00335533. doi: 10.2307/2937817. URL <https://academic.oup.com/qje/article-lookup/doi/10.2307/2937817>.
- 851 M. L. Weitzman. Why the Far-Distant Future Should Be Discounted at Its Lowest Possible
852 Rate. *Journal of Environmental Economics and Management*, 36(3):201–208, Nov. 1998. ISSN
853 00950696. doi: 10.1006/jem.1998.1052. URL <https://linkinghub.elsevier.com/retrieve/pii/S009506969891052X>.
- 855 M. L. Weitzman. A review of the stern review on the economics of climate change. *Journal of economic literature*, 45(3):703–724, 2007.
- 857 M. L. Weitzman. On Modeling and Interpreting the Economics of Catastrophic Climate Change.
858 *Review of Economics and Statistics*, 91(1):1–19, Feb. 2009. ISSN 0034-6535, 1530-9142. doi: 10.
859 1162/rest.91.1.1. URL <https://direct.mit.edu/rest/article/91/1/1-19/57734>.
- 860 M. L. Weitzman. GHG Targets as Insurance Against Catastrophic Climate Damages. *Journal of Public
861 Economic Theory*, 14(2):221–244, Mar. 2012. ISSN 10973923. doi: 10.1111/j.1467-9779.2011.01539.x.
862 URL <http://doi.wiley.com/10.1111/j.1467-9779.2011.01539.x>.
- 863 World Bank. State and Trends of Carbon Pricing 2021. Serial, World Bank, Washington, DC, May
864 2021. URL <https://openknowledge.worldbank.org/handle/10986/35620>.
- 865 T. P. Wright. Factors Affecting the Cost of Airplanes. *Journal of the Aeronautical Sciences*, 3(4):
866 122–128, Feb. 1936. ISSN 1936-9956. doi: 10.2514/8.155. URL <https://arc.aiaa.org/doi/10.2514/8.155>.
- 868 J. A. Yarmuth. Inflation Reduction Act of 2022, Aug. 2022. URL <https://www.congress.gov/bill/117th-congress/house-bill/5376>.

Online Appendix: Carbon Dioxide as a Risky Asset

Adam Michael Bauer^{*1}, Cristian Proistosescu^{2,3}, and Gernot Wagner⁴

¹*Department of Physics, University of Illinois Urbana-Champaign, 1110 W Green St Loomis Laboratory, Urbana, IL 61801, USA*

²*Department of Climate, Meteorology, and Atmospheric Sciences, University of Illinois Urbana-Champaign, 1301 W Green St, Urbana, IL 61801, USA*

³*Department of Earth Science and Environmental Change, University of Illinois Urbana-Champaign, 1301 W Green St, Urbana, IL 61801, USA*

⁴*Columbia Business School, 665 W 130th St, New York, NY 10027, USA*

Forthcoming in *Climatic Change*

March 13, 2024

Abstract

We develop a financial-economic model for carbon pricing with an explicit representation of decision making under risk and uncertainty that is consistent with the Intergovernmental Panel on Climate Change's sixth assessment report. We show that risk associated with high damages in the long term leads to stringent mitigation of carbon dioxide emissions in the near term, and find that this approach provides economic support for stringent warming targets across a variety of specifications. Our results provide insight into how a systematic incorporation of climate-related risk influences optimal emissions abatement pathways.

JEL: G0, G12, Q51, Q54

Keywords: Climate risk, climate policy, asset pricing, cost of carbon

^{*}Corresponding author email: adammb4@illinois.edu

¹ A Brief literature review

² There are three primary ways that risk and uncertainty are incorporated into climate-economic integrated assessment models. The first such approach is to augment DICE with stochastic components
³ and reframe the model into a dynamic stochastic optimal control problem. This approach has yielded
⁴ a number of fruitful insights (see, e.g., [Lemoine and Traeger \(2016a,b\)](#)). For example, the seminal work
⁵ of [Cai and Lontzek \(2019\)](#) show that the possibility of hitting a climate tipping point substantially increases
⁶ the SCC, and thus the stringency of optimal mitigation policy, using a continuous-time version
⁷ of DICE with many stochastic components.

⁹ Another approach is to formulate climate policy from the perspective of dynamic stochastic general equilibrium (DSGE) models. This approach was pioneered by [Golosov et al. \(2014\)](#), who derive a simple expression for the marginal externality damage from carbon emissions (analogously, the optimal carbon price or SCC). This expression shows that the optimal carbon price can be – in a stylized setting – decomposed into three contributing factors: (i) the discount rate, (ii) the elasticity of damage associated with a marginal ton of emissions, and (iii) the rate of depreciation of carbon stocks in the atmosphere. However, this study does not include temperature uncertainty, and utilizes a logarithmic utility, which causes the role of uncertainty to be substantially suppressed. [Van Den Bremer and Van Der Ploeg \(2021\)](#) extend the DGSE framework to include recursive preferences, finding that the influence of temperature and climate damage uncertainty increase the SCC. Similar conclusions were drawn by [Hambel et al. \(2021\)](#), whose formulation allows for multiple, additive climate shocks, as well as for considering the influence of climate change on both GDP levels and growth rates.

²¹ A third approach is to employ methods from financial economics to explore the influence of uncertainty on carbon prices. [Dietz et al. \(2018\)](#) utilize a simple analytic model derive the consumption-based capital asset pricing model “beta” ([Lucas, 1978](#)) for climate mitigation projects. They find that the sign of the “climate beta” is positive, and that the discounted expected net benefits of carbon emissions abatement are increasing in the “climate beta”. However, they do not utilize recursive preferences in their approach. [Lemoine \(2021\)](#) formulates a simple analytic expression that highlights the various channels of uncertainty associated with the SCC and signs each; the collective effect is positive. [Barnett et al. \(2020\)](#) build a dynamic structural model which includes decision making under uncertainty, nonlinear impulse response functions, and dynamic valuation, and find that the influence of uncertainty is multiplicative across economic and climate channels. Each of these contributions provide relatively simple – yet powerful – explanations, in financial economic terms, of how uncertainty influences optimal carbon pricing.

³³ **B Statement of optimization problem**

Put together, solving CAP6 is equivalent to solving the following optimization problem:

$$\max_{\{x_t\}_{t \in \{0, 1, \dots, T-1\}}} U_0(x_t), \quad (\text{B.1})$$

Such that : $x_t \in \mathbb{R}^+$, (B.2)

$$U_t = \left[(1 - \beta) c_t^\rho + \beta \left(\mathbb{E}_t [U_{t+1}^\alpha]^{1/\rho} \right) \right]^{1/\rho} \quad (\text{B.3})$$

$$U_T = \left(\frac{1 - \beta}{1 - \beta(1 + g)^\rho} \right)^{1/\rho} c_T, \quad (\text{B.4})$$

$$c_t = \bar{c}_t (1 - \kappa_t(x_t)) (1 - \mathcal{D}_t(\Psi_t, \theta_t)), \quad \forall t \in \{0, 1, \dots, T-1\} \quad (\text{B.5})$$

$$c_T = \bar{c}_T (1 - \mathcal{D}_T(\Psi_T, \theta_T)), \quad (\text{B.6})$$

$$\bar{c}_t = \bar{c}_0 (1 + g)^t, \quad (\text{B.7})$$

$$\Psi_t = \int_0^t E_\zeta d\zeta, \quad (\text{B.8})$$

$$\mathcal{D}_t(\Psi_t, \theta_t) = \sum_{\theta_t \in \Theta_t} P(\theta_T | \theta_t) \mathcal{D}_{tot}(\Psi_t, \theta_t) \quad (\text{B.9})$$

$$\kappa_t(x_t) = \kappa_{MACC}(x_t) (1 - \varphi_0 - \varphi_1 X_t)^{t-10}, \quad (\text{B.10})$$

$$X_t = \frac{\int_0^t x_\zeta E_\zeta d\zeta}{\Psi_t}, \quad (\text{B.11})$$

$$\beta = \frac{1}{1 + \delta} \quad (\text{B.12})$$

$$0 \leq P(\theta_T | \theta_t) \leq 1, \quad (\text{B.13})$$

$$\delta, \rho, \alpha, g, \varphi_0, \varphi_1, \tau_{DAC}, E_t \text{ given and positive}, \quad (\text{B.14})$$

$$\mathcal{D}_0(\Psi_t, \theta_t) = 0. \quad (\text{B.15})$$

³⁴ See the main text for details regarding functional forms, calibrations, and results after numerically
³⁵ solving the model.

³⁶ **C Prototypical model run**

³⁷ Given that our climate-economy model is unlike most other such models in the literature, an example
³⁸ of how each of the components laid out above interact in one model “run” is warranted. First, let us
³⁹ establish some important concepts and recurring values that will be essential for our understanding.
⁴⁰ We have chosen $T = 6$ decision periods. This implies that we have a total of $n := 2^T - 1 = 63$ decision
⁴¹ nodes in the tree. Decisions are made at times t such that $t \in \{2020, 2030, 2060, 2100, 2150, 2200\}$, and
⁴² an additional period (with no decisions being made) occurs at $t = 2250$ to establish the terminal period
⁴³ conditions. As the binomial tree is path dependent, it immediately follows that the number of unique
⁴⁴ paths through the tree is equal to the number of nodes in the *final* period, given by $n_f := 2^{T-1} = 32$.
⁴⁵ Any vector of length n (which represents the value of a given variable, say mitigation, at each *node* in
⁴⁶ the tree) can be readily translated into a set of *paths* of shape $n_f \times T$ through the tree (which represents
⁴⁷ the values of a given variable at the nodes in each *path* through the tree). Note that Figure 1 in the
⁴⁸ main text is a helpful visual guide for our entire discussion.

49 **Step 1: Simulate climate damages**

50 The first step is to simulate potential climate damages. This comes *before* agent utility is optimized,
51 as decisions about utility are made *within the context* of the landscape of potential damages. Once the
52 landscape of damages are calculated (and we will be more precise about what is meant by “landscape”
53 in our discussion below), then damages are interpolated in our utility calculations. Note that in the
54 following discussion $N_{MC} = 3 \times 10^6$ refers to the number of draws taken in our Monte Carlo samples
55 of TCRE and damage function parametric uncertainty.

56 Climate damages are simulated using the following prescription. First, we specify an emissions baseline
57 by choosing an SSP. Once specified, there is a range of possible cumulatively emitted CO₂ at each point
58 in time, depending on hypothetical agent mitigation policy. Let the maximum cumulative emissions
59 (associated with no mitigation) at a time t be represented by Ψ_t^* . Cumulative emissions Ψ_t therefore
60 always lie in the range $0 \leq \Psi_t \leq \Psi_t^*$. We discretize the range of potential cumulative emissions at each
61 point in time by applying a constant scaling $0 \leq m \leq 1$ to the SSP and computing damages for each
62 value of m . In our runs, we choose $M = 101$ values of m . To recapitulate: we choose a value of m such
63 that $0 \leq m \leq 1$, resulting in a time series of cumulative emissions $\Psi_t = m\Psi_t^*$ that is manifestly less
64 than or equal to the maximum permissible amount Ψ_t^* for all t .

65 For a given time series of cumulative emissions, the corresponding temperature change is uncertain
66 owing to the uncertainty in the TCRE. We draw N_{MC} samples of the TCRE from a rectified normal
67 distribution with best estimate and variance taken from Table 4 and evaluate (3.2), which results in
68 N_{MC} time series of global temperature change. For each temperature time series, we at random choose
69 a damage function (statistical, structural, or meta-analytic) and evaluate (2.6) for the chosen damage
70 function and the additional tipping points piece. The total damage is given by (2.7). This procedure
71 results in N_{MC} time series of climate damages. The climate damage time series are then ordered by
72 severity of the final period damages (thus establishing an orientation of the “fragility” dimension),
73 and grouped in N_{MC}/n_f sized bundles. An average is then taken over each bundle, resulting in n_f
74 time series of climate damages. The averaging procedure is necessary to make the simulated climate
75 damages congruent with the dimensionality of the binomial tree.

76 The procedure described above has resulted in a $n_f \times T$ matrix of climate damages, ordered from high
77 to low. Continuing for every value of m results in a $M \times n_f \times T$ *landscape* of climate damages. This is
78 coined as a landscape owing to its encapsulation of the potential extent of climate damages. The M -
79 dimension contains information about the extent of emissions; the T -dimension contains information
80 about the timing of damages; and the n_f -dimension contains the extent of climate damages based on
81 the uncertainty in TCRE and the damage function. With this landscape now calculated, we can turn
82 our attention to how the economic utility is maximized within it.

83 **Step 2: Utility maximization**

84 We optimize the economic utility given by (2.1) using a genetic algorithm (Goldberg, 1989). The genetic
85 algorithm is a stochastic optimization routine, where a set of random solution vectors are generated
86 and their “fitness” is determined. The vectors with high fitness are stored for the next round (they
87 “survive”), and vectors with low fitness are discarded (they “die”). The low fitness vectors are replaced
88 with another set of random vectors (the “offspring” of the more fit vectors) whose fitness is compared to
89 the incumbents’. This process continues until minimal changes in the highest fitness value are recorded
90 for a number of rounds; the vector corresponding to the highest fitness is then said to be the “optimal”
91 solution vector. The genetic algorithm is best suited for objective functions with unknown or difficult
92 to evaluate gradients, making it ideal for CAP6. In our use case, the randomly selected solution vectors
93 are mitigation vectors, and a given vector’s fitness is its 2020 economic utility. In what follows, allow
94 \vec{x} be a vector of mitigation values with length n .

95 EZ utility captures future risk by allowing the utility at time t be dependent on the utility at time $t + 1$
96 (see Eqn. (2.1)). Evaluating the utility must therefore begin at the final period, and is then evaluated
97 *backwards* to $t = 2020$. Thus, the first step is to evaluate the final period utility (2.2) where the final
98 period consumption is given by (2.5) for each final state node. (Recall there are $n_f = 32$ nodes in
99 the final period.) The assumed SSP and the mitigation vector \vec{x} are used to calculate the emissions
100 time series for every path through the tree, and thus the cumulative emissions at each end node. The
101 cumulative emissions are used in (2.8) to calculate the damages at each node.

102 For each node before the final period, the mitigation action *up to but not including* a given node is
103 used to calculate the cumulative emissions at that node. The cost of mitigation is found using (2.12),
104 and the damages are found using (2.8). These in tandem determine the consumption by (2.4). The
105 consumption and the following period utility are used in (2.1) to determine the utility. This continues
106 for each node, and each randomly generated vector, until the genetic algorithm finds the mitigation
107 vector with the highest utility.

108 Step 3: Visualize model output

109 The most fit mitigation vector \vec{x}^* translates into the output shown in Figures 5, 3, 6, 9, and 7 in the
110 following way. To calculate the cost, we apply (2.9) at each node, including the technological growth
111 prefactor found in (2.12). We calculate the expected mitigation using (2.13). We use \vec{x}^* to calculate the
112 emissions at each node, which readily translates into the concentrations at each node using (F.4) and
113 the *expected* warming at each node using (3.2) assuming the mean value of TCRE. Economic damages
114 for each node are calculated using \vec{x}^* in (2.8). Averaging over the cost, expected mitigation, emissions,
115 temperature, CO₂ concentrations, and damage amount in each period gives the time series shown in
116 Figures in the main text and the Online Appendix.

117 D Supplementary discussion: damage functions

118 In Table 1 we show the calibrated values and uncertainties for the free parameters in (2.6). Below, we
119 provide a technical description of how the values in Table 1 are computed.

120 D.1 Discussion of IPCC aggregate damage functions

121 D.1.1 Statistically estimated damage function

122 The statistically estimated damage function (Burke et al., 2018) builds on previous work involving the
123 nonlinear response of economic productivity to temperature (Burke et al., 2015), following methodolo-
124 gies laid out more generally in Carleton and Hsiang (2016). This damage function relies on the
125 specification of a certain horizon where damages set in, and choose the natural markers of 2049 and
126 2099 (mid-century and end of century, respectively). The mid-century and end of century estimates
127 are starkly different, as in this framework climate change slows economic growth, therefore requiring
128 sufficient time for damages to compound. Damages are also different depending on which SSP one
129 chooses; this owes to the fact that each SSP contains different assumptions around adaptation, techno-
130 logical growth, and so on. Finally, the warming levels represented in Burke et al. (2018) are relative to
131 a 1986–2005 baseline, *not* relative preindustrial temperature levels. The IPCC’s representation of this
132 damage function differs from the original publication in three ways: they only report end-of-century
133 estimates; they aggregate damage estimates across SSPs without indicating the differences between
134 each; and they report the temperature change as relative to preindustrial rather than to a 1986–2005
135 baseline.

Table 1: Fitted parameters for the damage function (2.6) based on Burke et al. (2018), Dietz et al. (2021) and Intergovernmental Panel on Climate Change (2022).

Damage function	$\bar{\varpi}_2 [K^{-2}]$	$\sigma_{\varpi_2} [K^{-2}]$	$\bar{\varpi}_1 [K^{-1}]$	$\sigma_{\varpi_1} [K^{-1}]$
Statistically estimated				
SSP1, mid-century	5.36×10^{-3}	7.13×10^{-4}	8.93×10^{-3}	1.12×10^{-3}
SSP2, mid-century	3.09×10^{-3}	4.76×10^{-4}	1.24×10^{-2}	1.90×10^{-3}
SSP3, mid-century	2.95×10^{-3}	4.74×10^{-4}	1.18×10^{-2}	1.89×10^{-3}
SSP4, mid-century	3.50×10^{-3}	7.14×10^{-4}	5.83×10^{-3}	1.19×10^{-3}
SSP5, mid-century	3.40×10^{-3}	5.20×10^{-4}	1.14×10^{-2}	1.75×10^{-3}
SSP1, end-of-century	-1.24×10^{-3}	2.49×10^{-4}	7.07×10^{-2}	1.42×10^{-2}
SSP2, end-of-century	-2.33×10^{-3}	4.75×10^{-4}	7.21×10^{-2}	1.47×10^{-2}
SSP3, end-of-century	-2.81×10^{-3}	5.93×10^{-4}	7.20×10^{-2}	1.52×10^{-2}
SSP4, end-of-century	-1.11×10^{-3}	3.42×10^{-4}	4.67×10^{-2}	1.43×10^{-2}
SSP5, end-of-century	-1.33×10^{-3}	3.45×10^{-4}	5.56×10^{-2}	1.45×10^{-2}
Structurally estimated	2.30×10^{-3}	8.53×10^{-4}	2.05×10^{-3}	7.59×10^{-4}
Meta analysis	6.85×10^{-3}	2.43×10^{-3}	2.98×10^{-4}	1.06×10^{-4}
Climate tipping points	4.8×10^{-1}	4×10^{-2}	-4×10^{-2}	1×10^{-2}

136 We correct these inconsistencies in our formulation to be consistent with the original publication. We
137 include explicitly the time dependence of this damage function in our simulated climate damages,
138 allowing for the decision periods of 2030 and 2060 to use the mid-century estimates and each decision
139 period from 2100 onward to use end of century estimates. This of course is not perfect, as damages
140 are expected to continue growing past 2100 in their framework, but we lack projection data to extend
141 their framework to longer time horizons. Therefore, our estimates of climate damages in the long run
142 are to be considered as conservative. We also change the fit to damage function data based on which
143 SSP we consider. Finally, we correct the temperature baseline by shifting the abscissa by ~ 0.8 °C to
144 correctly represent temperature anomalies relative to preindustrial levels.

145 A final qualifier to our use of this damage function is our parameterization of uncertainty. The un-
146 certainty range for these estimates is large, and net-benefits of climate change are not ruled out even
147 in the long term (though they are exceptionally rare). The extent of this uncertainty is largely driven
148 by the assumed economic response to climate change and the discount rate chosen in their model, and
149 no range is given for the estimates of economic damages for a given climate model’s projection; only
150 the median estimate is reported for each climate model. We also suppress climate model uncertainty
151 in their presented results so as to not double count climate uncertainty, resulting in a more narrow
152 uncertainty envelope for damages estimates. We present our formulation in Figure 3A, taking care to
153 allow uncertainty to broaden between 2049 and 2099, consistent with the original publication.

154 D.1.2 Structurally estimated damage function

155 In the case of the structurally estimated damage function (Rose et al., 2017), three IAMs’ (DICE (Nord-
156 haus, 1992), PAGE (Hope et al., 1993), and FUND (Tol, 1999)) output are aggregated to form a range
157 of climate damages estimates as a function of temperature. The central value of climate damages is
158 close to that of DICE–2023 (Barrage and Nordhaus, 2023). The uncertainty associated with this dam-
159 age function results from sampling the input parameter distribution of each IAM (Rose et al., 2017).
160 We present our formulation of this damage function based on IPCC data in Figure 3B.

161 D.1.3 Meta-analytic damage function

162 The meta-analytic damage function (Howard and Sterner, 2017) is derived from a synthesis of studies
163 found in the literature, where care was taken to account for duplicates of studies and methodology.
164 We use the preferred damage function from Howard and Sterner (2017), and assign an uncertainty
165 envelope which encompasses much of the spread in the data reported by the IPCC, see Figure 3C. One
166 limitation of this approach is that it is unclear if a set of damage estimates using different models and
167 estimation types can be joined together in this way to form one unified “damage function”; moreover,
168 it is also unclear if the uncertainty found in the data can truly be labeled as “parametric” or simply a
169 by-product of disagreements in the literature.

170 D.1.4 Synthesis

171 The inability to properly compare damage estimates across studies and methodologies led WGI to
172 conclude that a reliable range of damage estimates could not be determined; there is no single ‘correct’
173 damage function that we can specify in this work (Intergovernmental Panel on Climate Change, 2022).
174 We resolve this issue by taking a conservative approach and sampling all of the damage functions
175 mentioned above with equal probabilities; in this way, we remain agnostic about which damage function
176 is the ‘correct’ one, and sample the space of possible damage functions in addition to uncertainty
177 inherent to a specific climate damage estimation methodology.

Despite the issues with individual damage functions described above, our approach to sampling all available damage functions has the benefit that, at minimum, we sample a variety of damage function shapes and scales. The statistically estimated damage function has a concave shape at end-of-century. Furthermore, this damage function is time dependent, capturing the impact of climate change impacting economic growth; this has been shown to be an important factor in climate policy (Moore and Diaz, 2015). The structurally estimated damage function, in contrast, is convex, with low damages in the short run which slowly rise in temperature. Finally, the meta-analytic damage function is also convex, but rises much faster than the structurally estimated damage function.

D.2 Damage function calibration

We fit the damage function data in the following way. For each damage function, we require that the concavity of the damage function is preserved, i.e., $\partial^2\mathcal{D}/\partial T'^2 \geq 0$, depending on the damage function being considered. To solve for the damage function coefficients as presented in (2.6), we require knowing the damages for two data points, generically labeled as (T_1, \mathcal{D}_1) and (T_2, \mathcal{D}_2) . Then we can write

$$\mathcal{D}_1 = T_1(\varpi_2 T_1 + \varpi_1), \quad (\text{D.1})$$

$$\mathcal{D}_2 = T_2(\varpi_2 T_2 + \varpi_1), \quad (\text{D.2})$$

and, solving the above for ϖ_1 and ϖ_2 , results in

$$\varpi_1 = \frac{\mathcal{D}_1 T_2^2 - \mathcal{D}_2 T_1^2}{T_2 T_1 (T_2 - T_1)}, \quad (\text{D.3})$$

$$\varpi_2 = \frac{\mathcal{D}_2 T_1 - \mathcal{D}_1 T_2}{T_2 T_1 (T_2 - T_1)}. \quad (\text{D.4})$$

Having established the mean state, we can now introduce uncertainty into (D.3) and (D.4). We do so by allowing \mathcal{D}_1 to be uncertain, assigning it a Gaussian distribution $\tilde{\mathcal{D}}_1$ with mean $\bar{\mathcal{D}}_1$ and standard deviation $\sigma_{\mathcal{D}_1}$. We link this to a distribution of \mathcal{D}_2 by invoking the condition $\partial^2\mathcal{D}/\partial T'^2 \geq 0$, immediately resulting in the condition $\varpi_2 \geq 0$. Using (D.4), we arrive at

$$\tilde{\mathcal{D}}_2 \geq \tilde{\mathcal{D}}_1 \left(\frac{T_2}{T_1} \right). \quad (\text{D.5})$$

Eqn. (D.5) is generic for any damage function, but our model, we want either a concave up or concave down damage function. To accomplish this, we include an additional factor $\Lambda > 0$ to (D.5) such that the inequality is ensured, i.e.,

$$\tilde{\mathcal{D}}_2 = \Lambda \tilde{\mathcal{D}}_1 \left(\frac{T_2}{T_1} \right), \quad \text{such that } \Lambda \geq 1. \quad (\text{D.6})$$

Therefore, if $\Lambda > 1$, we have a concave up damage function, and if $\Lambda < 1$, we have a concave down damage function. Setting $T_1 = 3^\circ\text{C}$ and $T_2 = 10^\circ\text{C}$, we fit values for $\bar{\mathcal{D}}_1$, $\sigma_{\mathcal{D}_1}$, and Λ to each set of damage function data resulting in the values presented in Table 1. See Table 2 for the values of our calibration coefficients.

E Supplementary discussion: cost of mitigation

E.1 Marginal abatement cost curve alternative calibrations

As a sensitivity test of our marginal abatement cost curve (MACC), we increased the cost of each mitigation option by one cost bracket, eliminating the zero-cost mitigation options (i.e., “free lunch” options) that the IPCC reports in their WGIII report. The resulting cost figure is in Figure 1.

Table 2: Fitted parameters for the damage function calibration equation (D.6) based on Burke et al. (2018), Dietz et al. (2021) and Intergovernmental Panel on Climate Change (2022).

Damage function	$\bar{\mathcal{D}}_1 [-]$	$\sigma_{\mathcal{D}_1} [-]$	Λ
Statistically estimated			
SSP1, mid-century	0.075	0.01	2.5
SSP2, mid-century	0.065	0.01	2.0
SSP3, mid-century	0.062	0.01	2.0
SSP4, mid-century	0.049	0.01	2.5
SSP5, mid-century	0.065	0.01	2.1
SSP1, end-of-century	0.2	0.04	0.87
SSP2, end-of-century	0.195	0.04	0.75
SSP3, end-of-century	0.19	0.04	0.69
SSP4, end-of-century	0.13	0.04	0.82
SSP5, end-of-century	0.155	0.04	0.82
Structurally estimated	0.027	0.01	2.8
Meta analysis of climate damages	0.063	0.022	3.3

Table 3: Fitted coefficients for (2.9), the cost of abating all emissions, $\tau_a := \tau(x = 1)$, and the percent of consumption required to abate all emissions, $\kappa_a := \kappa_{MACC}(x = 1)$, based on AR6 WGIII data for each SSP in our ‘main specification’ and our “no free lunches” alternative calibration. All dollar values are in 2020 \$USD.

SSP	ξ	$\tau_0 [\$/tCO_2\text{-eq}^{-1}]$	$\tau_a [\$/tCO_2\text{-eq}^{-1}]$	$\kappa_a [\%]$
<i>Main specification</i>				
1	1.9	27.5	153.88	3.0
2	2.4	27.5	264.09	5.9
3	2.9	27.5	457.57	11.3
4	2.5	27.5	292.15	6.69
5	3.0	27.5	526.58	13.2
<i>“No free lunches”</i>				
1	1.8	58.9	297.42	6.1
2	2.3	58.9	528.58	11.9
3	2.8	58.9	909.69	22.5
4	2.3	58.9	528.58	13.4
5	2.9	58.9	1011.56	26.3

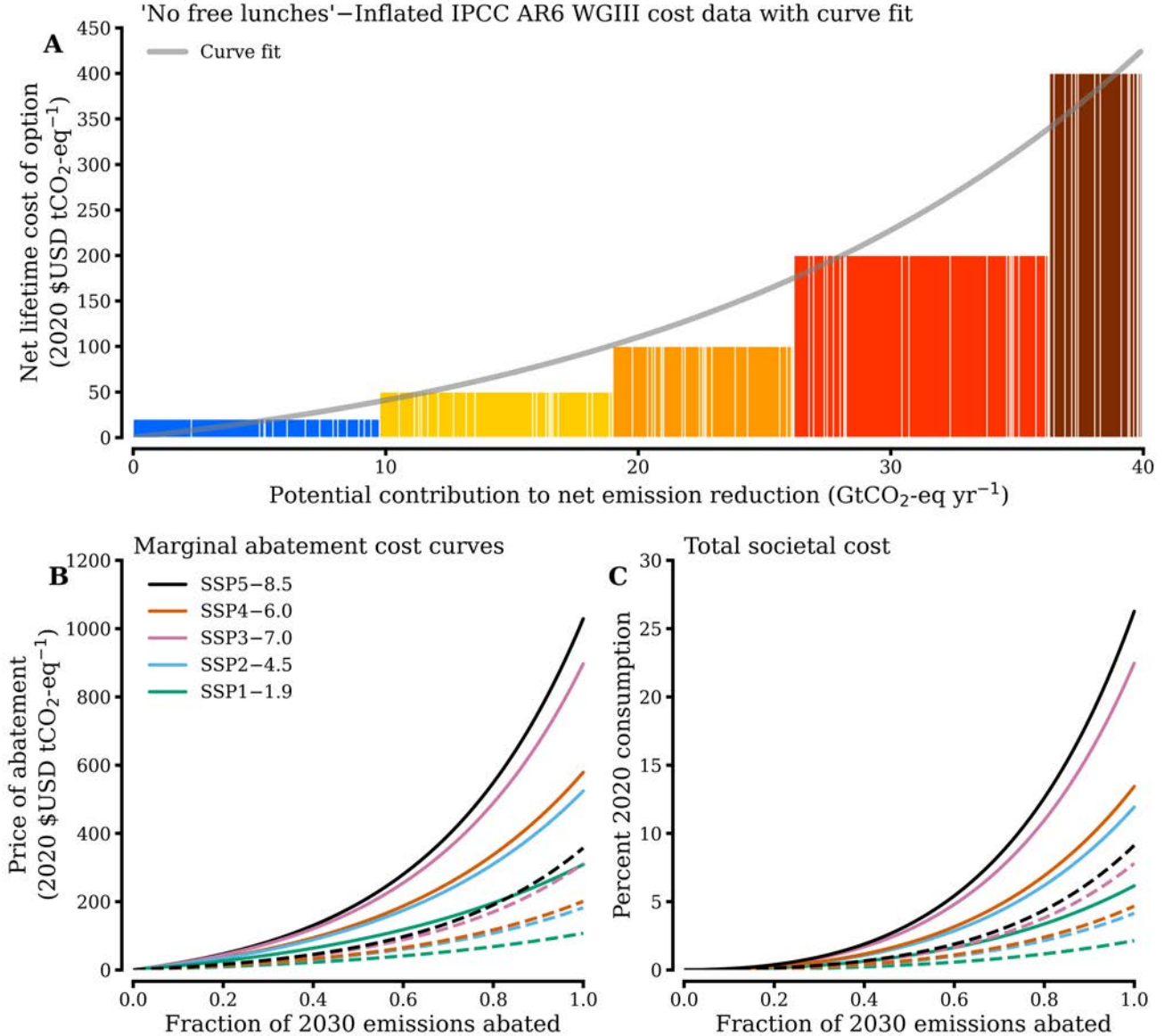


Figure 1: Panel A shows the mitigation potential and cost for each methodology given by the IPCC using their WGIII data after adjusting for the “no free lunches” calibration. Blue bars represent the \$0-\$20 range, yellow is \$20-\$50, orange is \$50-\$100, red is \$100-\$200, and maroon is our new cost bracket \$400. Our curve fit is in grey. Panel B shows the fitted marginal abatement cost curves and panel C shows the total cost to society. In panels B–C, solid lines correspond to 2030, while dashed lines are cost curves in 2100, assuming an exogenous technological growth rate of 1.5% and no endogenous technological growth.

203 As another sensitivity test of our marginal abatement cost curve (MACC), we cut out the < \$0
 204 abatement potential reported by the IPCC WGIII data and fit a curve to the nonzero cost options.
 205 The resulting cost figure is in Figure 2. Note that this marginal abatement cost curve (MACC) results
 206 in costs that are lower than the “no free lunches” calibration. Hence, we do not present Climate Asset
 207 Pricing model – AR6 runs with this cost curve specified, as the results will be simple interpolations
 208 between the main specification results and the “no free lunches” results.

209 E.2 Limitations of our cost of abatement approach

210 A major qualification to our results regards two assumptions in our cost of CO₂ abatement parame-
 211 terization. The first major assumption is that abatement technologies are essentially instantly able to
 212 be deployed; we do not capture real-world inertia, represented in other energy systems IAMs, that cap
 213 the rate of decarbonization owing to the delayed availability of abatement technologies, stranded as-
 214 sets, limited construction times, and other factors (Ha-Duong et al., 1997; Richels and Blanford, 2008;
 215 Vogt-Schilb et al., 2018). This limitation, however, is common in other IAMs such as DICE (Nordhaus,
 216 2017) which have been widely used to study optimal climate-economic policy (Committee on Assessing
 217 Approaches to Updating the Social Cost of Carbon et al., 2017). Secondly, our MACC assumes that
 218 the sacrificed consumption to abate CO₂ emissions does not feedback on other aspects of the economy,
 219 such as growth or productivity (Hogan and Jorgenson, 1991). Including a more sophisticated abate-
 220 ment cost parameterization (i.e., through representing investments in abatement capital explicitly) or
 221 the feedback of mitigation policy on growth would be an interesting direction for future work. These
 222 limitations provide important context for our results.

223 E.3 Full derivation of total cost to society, Eqn. (2.10)

224 First, assume a representative agent optimizes consumption $c(\tau)$ such that $dc(\tau)/d\tau = -E(x(\tau)) =$
 225 $-E(\tau)$, where we have dropped the dependence of the emissions on mitigation action for clarity. Then
 226 by simple integration the consumption is given by

$$c(\tau) = \bar{c} - \underbrace{\int_0^\tau E(\zeta)d\zeta}_{=:K(\tau)}, \quad (\text{E.1})$$

227 where $\bar{c} > 0$ is the baseline endowed consumption and $K(\tau)$ is the cost to society in monetary units
 228 (i.e., dollars). Eqn. (E.1) would be correct if the government was to waste the entirety of the policy
 229 proceeds, given by $E(\tau)\tau$. We instead assume that the proceeds are refunded in a lump sum (Mankiw
 230 et al., 2009), thus requiring an alteration to $K(\tau)$ such that

$$K(\tau) = \int_0^\tau E(\zeta)d\zeta - E(\tau)\tau. \quad (\text{E.2})$$

231 The lump sum refund does not allow for CO₂ tax proceeds to be used to decrease distortionary taxes
 232 unrelated to CO₂ emissions; this would lower the *net* cost of CO₂ even further (Goulder, 1995; Jorgen-
 233 son, 2013). Rewriting the emissions as $E(\tau) = E_0(1 - x(\tau))$ where E_0 is the (SSP-dependent) 2030
 234 emissions in GtCO₂ yr⁻¹, we have

$$K(\tau) = E_0 \left(\tau x(\tau) - \int_0^\tau x(\zeta)d\zeta \right). \quad (\text{E.3})$$

235 Note that E_0 is the 2030 emissions for consistency with the cost data presented by WGIII. Now
 236 using (2.9) and its inverse in (E.3), carrying out the integral, and dividing by 2020 consumption results

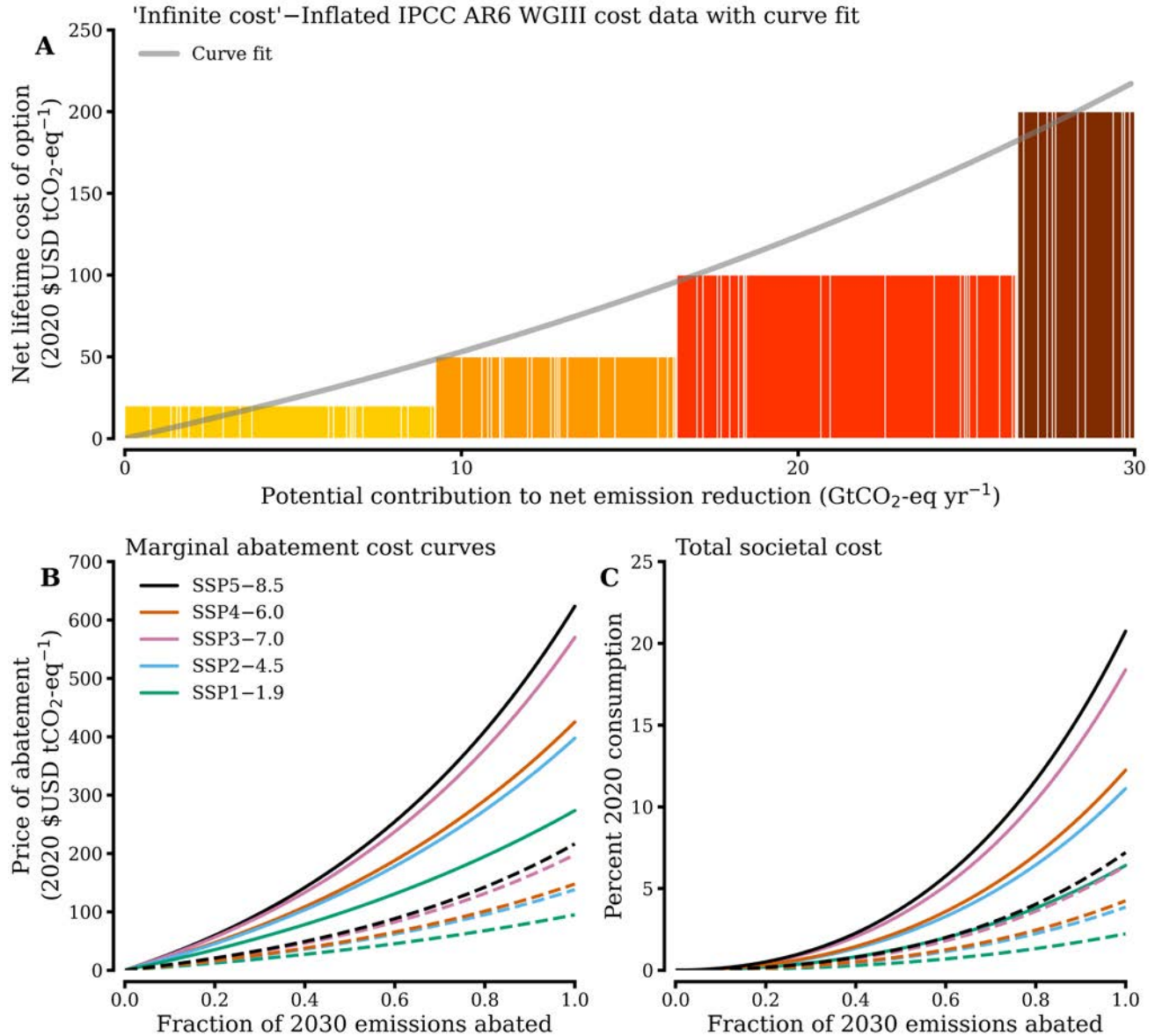


Figure 2: Panel A shows the mitigation potential and cost for each methodology given by the IPCC using their WGIII data after adjusting for the “infinite cost” calibration. Yellow bars are the \$0-\$20 range, orange is \$20-\$50, red is \$50-\$100, and maroon is \$100-\$200. Our curve fit is in grey. Panel B shows the fitted marginal abatement cost curves and Panel C shows the total cost to society. In panels B–C, solid lines correspond to 2030, while dashed lines are cost curves in 2100, assuming an exogenous technological growth rate of 1.5% and no endogenous technological growth.

Table 4: Values of fitting coefficients a_i and timescales τ_i used in (F.2) (taken from Joos et al. (2013)), as well as the best estimate and standard deviation of TCRE (taken from Intergovernmental Panel on Climate Change (2021) and Damon Matthews et al. (2021)).

Fitting Coefficient		Timescale [years]	
a_0	0.2173	τ_1	394.4
a_1	0.2240	τ_2	36.54
a_2	0.2824	τ_3	4.304
a_3	0.2763		
TCRE Parameters			
$\bar{\lambda} = 0.45 \text{ } ^\circ\text{C (1000 GtCO}_2)^{-1}$		$\sigma_\lambda = 0.18 \text{ } ^\circ\text{C (1000 GtCO}_2)^{-1}$	
$\bar{f}_{nc} = 0.14$		$\sigma_{f_{nc}} = 0.11$	
$\bar{\lambda}_{eff} = 0.52 \text{ } ^\circ\text{C (1000 GtCO}_2)^{-1}$		$\sigma_{\lambda_{eff}} = 0.21 \text{ } ^\circ\text{C (1000 GtCO}_2)^{-1}$	

237 in the total cost to society in terms of fractional 2020 consumption loss, given by $\kappa_{MACC}(x)$, as

$$\kappa_{MACC}(x) = \frac{E_0 \tau_0}{c_{2020}} \left(\frac{e^{\xi x} - 1}{\xi} - x \right), \quad (\text{E.4})$$

238 where c_{2020} is the 2020 global consumption in billions of 2020 \$USD. This completes our derivation.

239 F Supplementary discussion: climate model

240 In Table 5 we compare the average warming levels using our effective TCRE approach and the weighted
241 model averages presented by the IPCC in AR6.

242 F.1 Carbon cycle model

243 For a given emission time series the corresponding CO₂ concentration time series can be found by
244 convolving emissions with the impulse response function (IRF) of a pulse of CO₂ emissions, denoted
245 as $\mathcal{I}(t)$, such that

$$\mathcal{C}_E(t) = E(t) * \mathcal{I}(t). \quad (\text{F.1})$$

246 In Joos et al. (2013), it is shown that the IRF for a pulse of CO₂ can be sufficiently represented by a
247 superposition of exponentials, given by

$$\mathcal{I}(t) := a_0 + a_1 e^{-t/\tau_1} + a_2 e^{-t/\tau_2} + a_3 e^{-t/\tau_3}. \quad (\text{F.2})$$

248 See Table 4 for the numerical values of the fitting coefficients a_i and timescales τ_i in (F.2).

249 The final component of the concentration time series accounts for pre-2020 CO₂ that is present in the
250 atmosphere when an agent begins emitting. This ensures that our carbon cycle model not only acts to
251 take new CO₂ out of the atmosphere, but continues to remove CO₂ from past emissions. To account
252 for this extra CO₂ in the atmosphere, we make the assumption that the majority of CO₂ before 2020
253 is old, such that the time it has been in the atmosphere is much greater than τ_2 . This implies that

Table 5: Shown are the central estimate and the 5%-95% range of warming levels in three time periods, for three emissions baselines, using our effective TCRE approach and what is reported by the IPCC in their Table 4.5.

Time period	Effective TCRE range ($^{\circ}\text{C}$)	AR6 range ($^{\circ}\text{C}$)
SSP2–4.5		
Near-term: 2021–2040	1.5 (1.3 to 1.6)	1.5 (1.2 to 1.8)
Mid-term: 2041–2060	1.9 (1.5 to 2.4)	2.0 (1.6 to 2.5)
Long-term: 2081–2100	2.6 (1.7 to 3.5)	2.7 (2.1 to 3.5)
SSP3–7.0		
Near-term: 2021–2040	1.5 (1.3 to 1.7)	1.5 (1.2 to 1.8)
Mid-term: 2041–2060	2.1 (1.6 to 2.7)	2.1 (1.7 to 2.6)
Long-term: 2081–2100	3.6 (2.1 to 5.1)	3.6 (2.8 to 4.6)
SSP5–8.5		
Near-term: 2021–2040	1.5 (1.3 to 1.7)	1.6 (1.3 to 1.9)
Mid-term: 2041–2060	2.3 (1.6 to 2.9)	2.4 (1.9 to 3.0)
Long-term: 2081–2100	4.6 (2.4 to 6.8)	4.4 (3.3 to 5.7)

254 there is a constant fraction that remains, and a piece that is still decaying. Hence, the remaining CO₂
 255 in the atmosphere is given by

$$\mathcal{C}_{\text{pre}-2020}(t) = \mathcal{C}_{2020} \left(\frac{a_0 + a_1 e^{-t/\tau_1}}{a_0 + a_1} \right), \quad (\text{F.3})$$

256 where $\mathcal{C}_{2020} = 420.87$ ppm.¹ Therefore, we can write the total carbon concentrations time series for a
 257 given individual as

$$\mathcal{C}(t) = \mathcal{C}_{2020} \left(\frac{a_0 + a_1 e^{-t/\tau_1}}{a_0 + a_1} \right) + E(t) * \mathcal{I}(t). \quad (\text{F.4})$$

258 We note that (F.4) is used only to compute carbon concentrations as a result of optimal policy in
 259 Figures 5–8; we do not utilize carbon concentrations in our optimization routine, as our temperature
 260 parameterization relies on cumulative emissions only.

261 G Supplementary discussion: discount rate calibration

262 In Table 6 we show the term structures of the discount rates used in our featured runs. In Table 7 we
 263 show the ranges of parameters that are sampled in our ensemble runs.

Table 6: Term structures for each discount rate in featured CAP6 runs.

Discount rate [%]	δ [%]	η
1.5	0.1	0.93
2	0.2	1.20
2.5	0.5	1.42
3	0.8	1.53

Table 7: Ranges of values for each model parameter sampled in the ensemble runs.

Parameter	Symbol	Range
Risk aversion	ψ	3 – 15
Elasticity of intertemporal substitution	σ	0.55 – 1.08
Pure rate of time preference	δ	0.1% – 1.47%
Exogenous rate of technological growth	φ_0	0% – 3%
Endogenous rate of technological growth	φ_1	0% – 3%

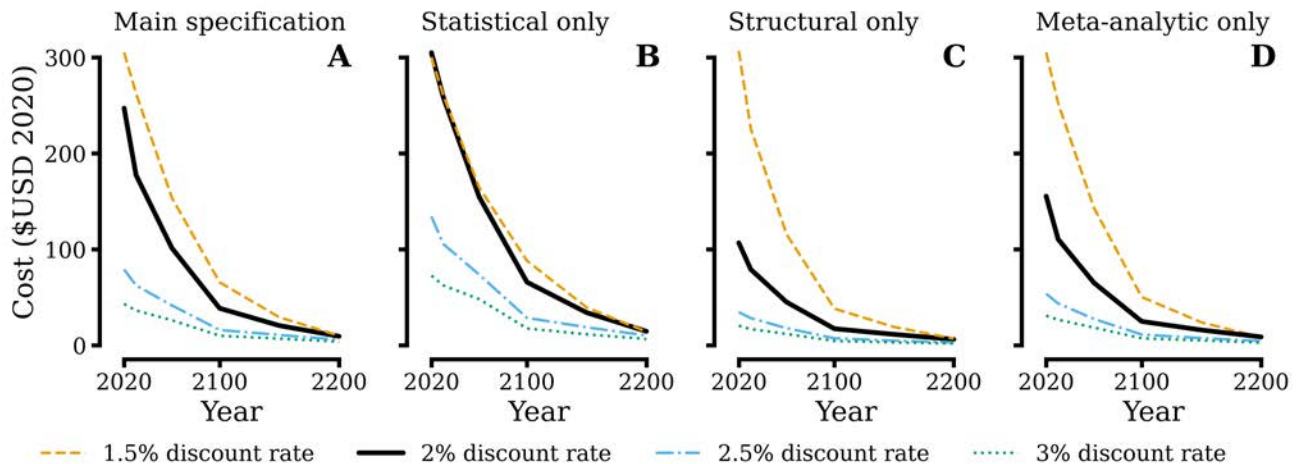


Figure 3: Price paths for each damage function. All damage functions are sampled in panel A.

264 **H Isolating individual damage functions**

265 We isolate the influence of each damage function on carbon price paths in Figure 3 by isolating a single
266 damage function and re-running our featured model runs. For comparison, we also provide our featured
267 runs in panel 3A. Beginning with the statistically estimated damage function, we find that prices are
268 higher in the near term in comparison to the other damage functions, with the exception of the 1.5%
269 discount rate run. By comparison, running CAP6 with a convex damage function (i.e., the structural
270 and meta-analytic damage functions) results in lower prices in the near term, with the exception of the
271 1.5% discount rate runs. This shows that for sufficiently low discount rates, individual preferences can
272 supercede the specifics of model components in ‘optimal’ policy considerations.

273 **I Regression analysis**

274 Regression coefficients in Figure 8 are calculated by fitting a linear regression between each parameter
275 value and carbon costs. The one exception is technological growth, which is time dependent and given
276 by

$$\varphi := \varphi_0 + \varphi_1 X_t. \quad (\text{I.1})$$

277 In 2100 and later, technological change is nonlinearly related to carbon costs. We therefore fit a
278 quadratic to carbon costs as a function of total technological growth from 2100 on. Figures 4, 5, 6,
279 and 7 show the intermediate step in computing the results shown in Figure 8.

280 **J Impact of Epstein-Zin risk aversion on prices**

281 Shown in Figure 8 is the influence of changing the Epstein-Zin risk aversion parameter, ψ , on CO₂
282 prices. Increasing (decreasing, resp.) ψ causes an increase (decrease, resp.) in the optimal carbon tax,
283 consistent with other studies (e.g., Cai and Lontzek, 2019).

284 **K Including learning by doing**

285 We run CAP6 with learning by doing (LbD) included for both our main specification and “no free
286 lunches” MACC in Figure 9. Note we use a 2% discount rate for each curve in Figure 9, $\varphi_1 = 1.5\%$
287 when LbD is enabled, and all other calibration parameters are the same as in our ‘main specification’
288 runs above. We find that including LbD causes a relatively minor change in the the present-day carbon
289 price for both MACC, and lowers the overall cost burden of the optimal abatement policy (i.e., the
290 integrated cost over time). This is owed to prices declining faster as consumption is spent on mitigation,
291 thus enabling more abatement in the near-term for cheaper costs. Furthermore, enabling LbD lowers
292 the expected optimal warming by ~ 0.05 °C in 2100 for both MACCs. For the ‘main specification’
293 MACC, warming in 2200 is lower by ~ 0.1 °C, whereas for the “no free lunches” MACC 2200 warming
294 is lower by ~ 0.12 °C.

295 A notable result from this exercise is that by including LbD effects, the 2% discount rate policy
296 with our ‘main specification’ cost curve stays below the 1.5 °C warming target in 2200; recall this
297 threshold was exceeded when LbD was excluded. Hence, we can expect that the feasibility of reaching
298 the warming targets set forth in Paris are highly sensitive to such outcomes; given that the rate of
299 endogenous technological change is difficult to empirically ground, this represents a significant source
300 of uncertainty in policy projections and a target for future research.

¹Taken from <https://keelingcurve.ucsd.edu/>

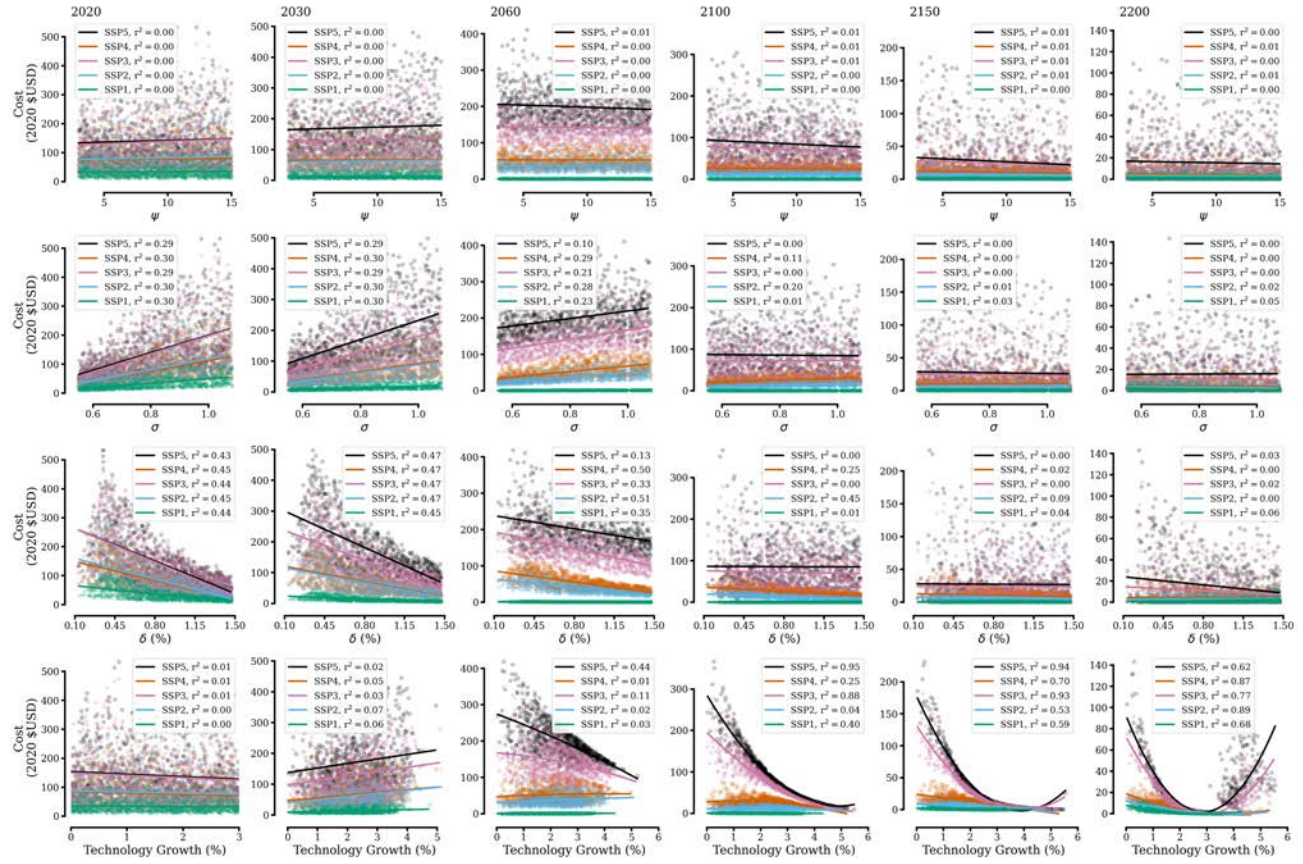


Figure 4: In each row, we plot the regression of each parameter against carbon costs in that period. r^2 values are given for each regression in the legend of each panel.

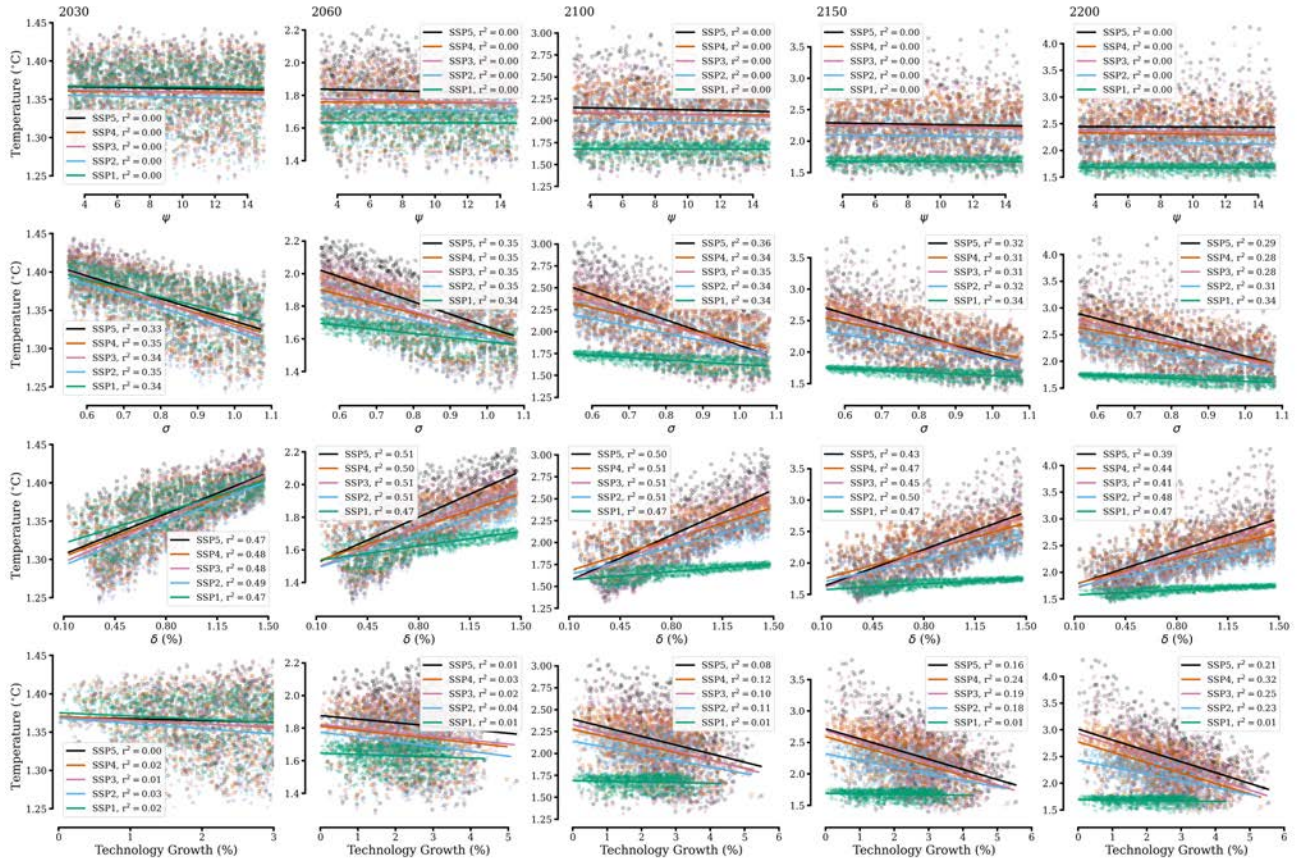


Figure 5: In each row, we plot the regression of each parameter against temperature in that period. r^2 values are given for each regression in the legend of each panel.

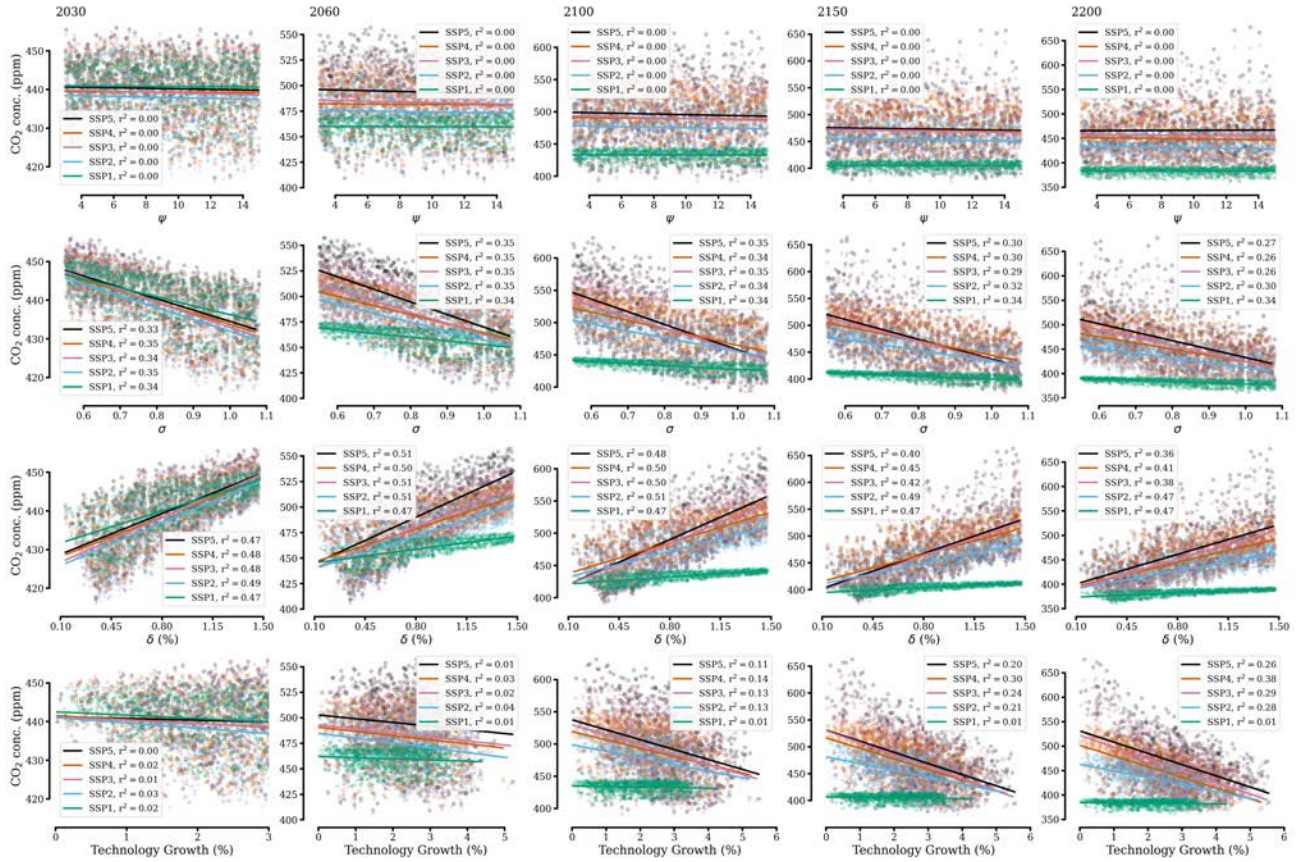


Figure 6: In each row, we plot the regression of each parameter against CO₂ concentrations in that period. r^2 values are given for each regression in the legend of each panel.

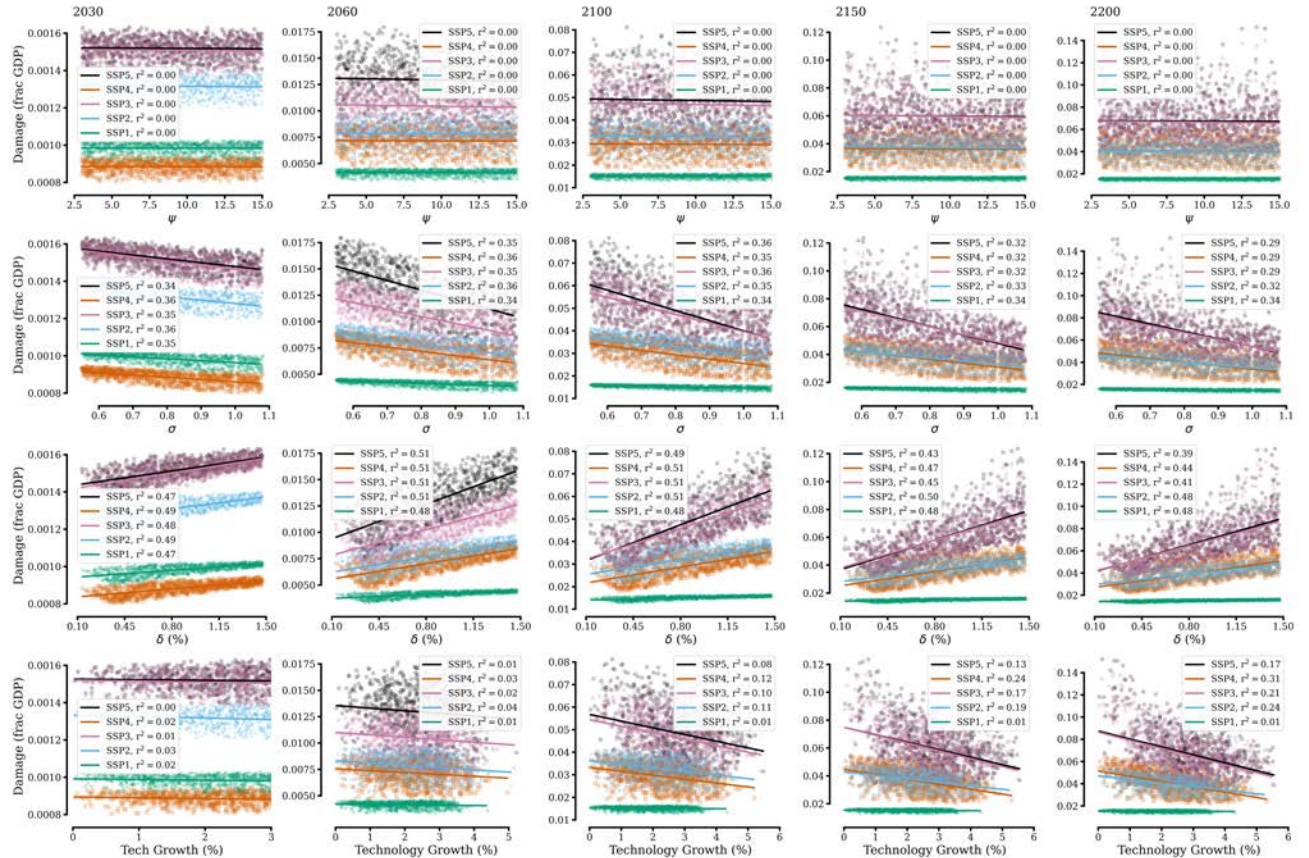


Figure 7: In each row, we plot the regression of each parameter against economic damages in that period. r^2 values are given for each regression in the legend of each panel.

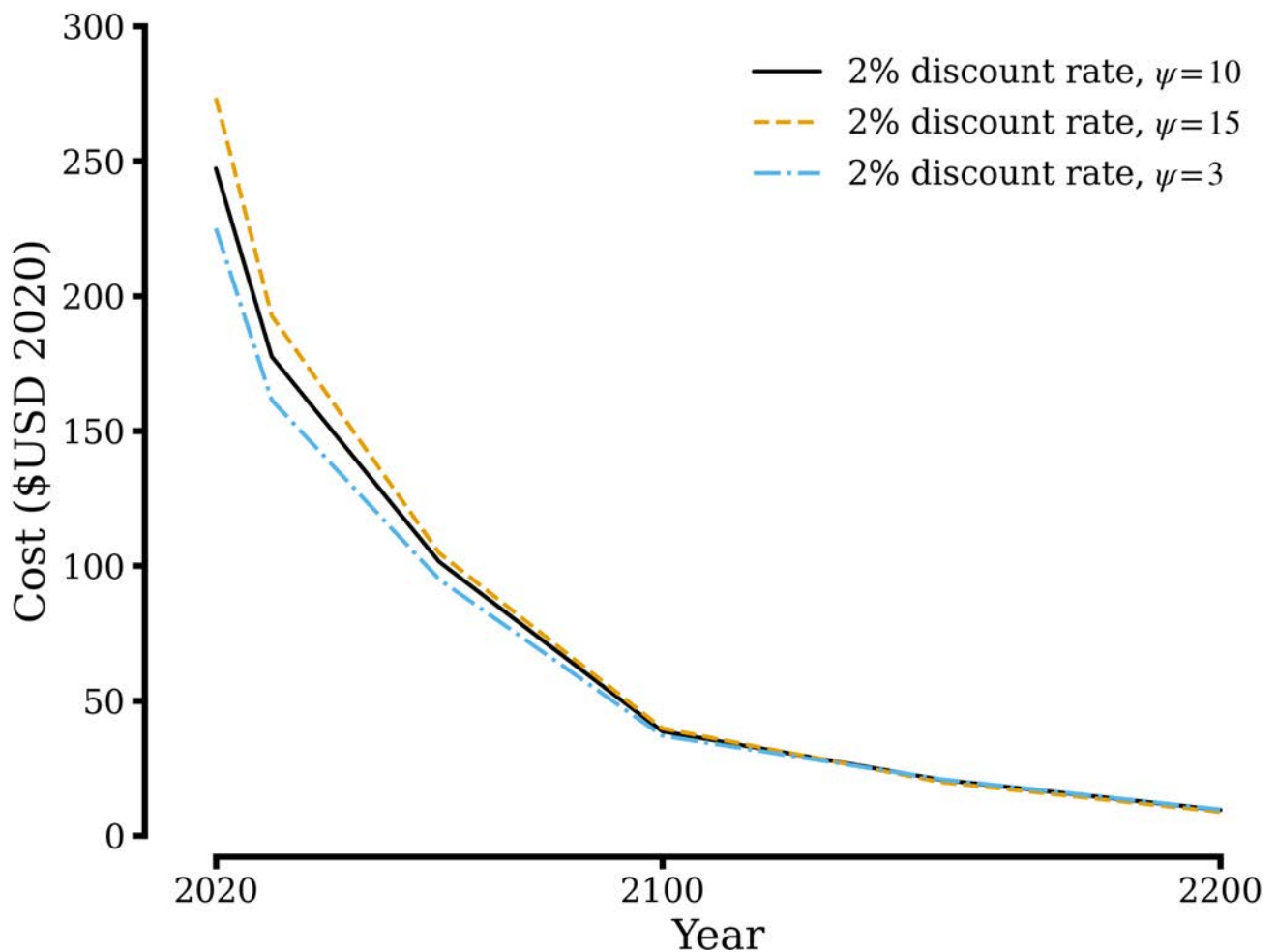


Figure 8: Shown is the resulting price path for different choices of risk aversion, holding all other model inputs constant in our preferred calibration.

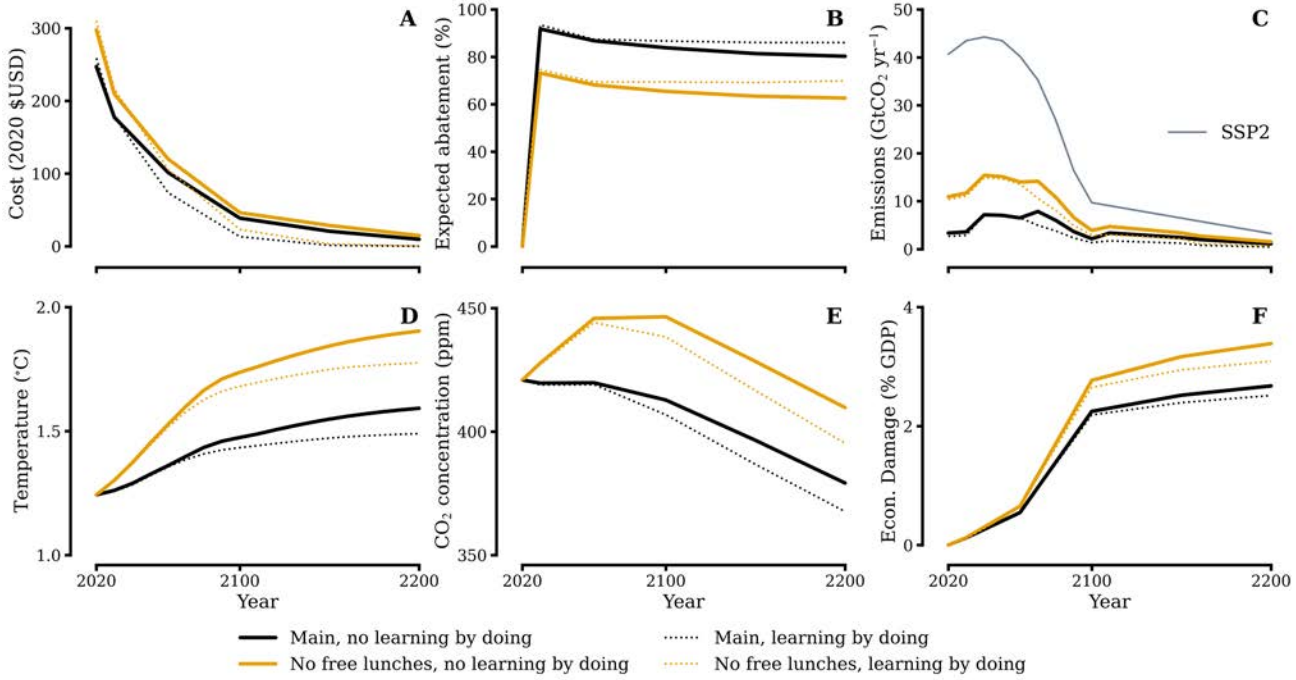


Figure 9: We show model output using our preferred 2% discount rate and toggling which MACC we use ('main' or "no free lunches") with or without learning by doing.

Note: Learning by doing implies that $\varphi_1 = 1.5\%$; no learning by doing corresponds to $\varphi_1 = 0\%$. All other parameters are the same as in our main specification.

301 References

- 302 M. Barnett, W. Brock, and L. P. Hansen. Pricing Uncertainty Induced by Climate Change. *The
303 Review of Financial Studies*, 33(3):1024–1066, Mar. 2020. ISSN 0893-9454, 1465-7368. doi: 10.1093/
304 rfs/hhz144. URL <https://academic.oup.com/rfs/article/33/3/1024/5735312>.
- 305 L. Barrage and W. Nordhaus. Policies, Projections, and the Social Cost of Carbon: Results from the
306 DICE-2023 Model. Technical Report w31112, National Bureau of Economic Research, Cambridge,
307 MA, Apr. 2023. URL <http://www.nber.org/papers/w31112.pdf>.
- 308 M. Burke, S. M. Hsiang, and E. Miguel. Global non-linear effect of temperature on economic production.
309 *Nature*, 527(7577):235–239, Nov. 2015. ISSN 0028-0836, 1476-4687. doi: 10.1038/nature15725. URL
310 <http://www.nature.com/articles/nature15725>.
- 311 M. Burke, W. M. Davis, and N. S. Diffenbaugh. Large potential reduction in economic damages under
312 UN mitigation targets. *Nature*, 557(7706):549–553, May 2018. ISSN 0028-0836, 1476-4687. doi:
313 10.1038/s41586-018-0071-9. URL <http://www.nature.com/articles/s41586-018-0071-9>.
- 314 Y. Cai and T. S. Lontzek. The Social Cost of Carbon with Economic and Climate Risks. *Journal of
315 Political Economy*, 127(6):2684–2734, Dec. 2019. ISSN 0022-3808, 1537-534X. doi: 10.1086/701890.
316 URL <https://www.journals.uchicago.edu/doi/10.1086/701890>.
- 317 T. A. Carleton and S. M. Hsiang. Social and economic impacts of climate. *Science*, 353(6304):aad9837,
318 Sept. 2016. ISSN 0036-8075, 1095-9203. doi: 10.1126/science.aad9837. URL <https://www.science.org/doi/10.1126/science.aad9837>.

- 320 Committee on Assessing Approaches to Updating the Social Cost of Carbon, Board on Environmental
321 Change and Society, Division of Behavioral and Social Sciences and Education, and National
322 Academies of Sciences, Engineering, and Medicine. *Valuing Climate Changes: Updating Estimation*
323 of the Social Cost of Carbon Dioxide. National Academies Press, Washington, D.C., 2017. ISBN
324 9780309454209. doi: 10.17226/24651. URL <https://www.nap.edu/catalog/24651>.
- 325 H. Damon Matthews, K. B. Tokarska, J. Rogelj, C. J. Smith, A. H. MacDougall, K. Haustein,
326 N. Mengis, S. Sippel, P. M. Forster, and R. Knutti. An integrated approach to quantifying uncer-
327 tainties in the remaining carbon budget. *Communications Earth & Environment*, 2(1):7, Jan. 2021.
328 ISSN 2662-4435. doi: 10.1038/s43247-020-00064-9. URL <https://www.nature.com/articles/s43247-020-00064-9>.
- 330 S. Dietz, C. Gollier, and L. Kessler. The climate beta. *Journal of Environmental Economics and*
331 *Management*, 87:258–274, Jan. 2018. ISSN 00950696. doi: 10.1016/j.jeem.2017.07.005. URL <https://linkinghub.elsevier.com/retrieve/pii/S0095069617304734>.
- 333 S. Dietz, J. Rising, T. Stoerk, and G. Wagner. Economic impacts of tipping points in the climate
334 system. *Proceedings of the National Academy of Sciences*, 118(34):e2103081118, Aug. 2021. ISSN
335 0027-8424, 1091-6490. doi: 10.1073/pnas.2103081118. URL <https://pnas.org/doi/full/10.1073/pnas.2103081118>.
- 337 D. E. Goldberg. *Genetic algorithms in search, optimization, and machine learning*. Addison-Wesley
338 Pub. Co, Reading, Mass, 1989. ISBN 9780201157673.
- 339 M. Golosov, J. Hassler, P. Krusell, and A. Tsyvinski. Optimal Taxes on Fossil Fuel in General
340 Equilibrium. *Econometrica*, 82(1):41–88, 2014. ISSN 0012-9682. doi: 10.3982/ECTA10217. URL
341 <http://doi.wiley.com/10.3982/ECTA10217>.
- 342 L. H. Goulder. Environmental taxation and the double dividend: A reader’s guide. *International Tax*
343 and *Public Finance*, 2(2):157–183, Aug. 1995. ISSN 0927-5940, 1573-6970. doi: 10.1007/BF00877495.
344 URL <http://link.springer.com/10.1007/BF00877495>.
- 345 M. Ha-Duong, M. J. Grubb, and J.-C. Hourcade. Influence of socioeconomic inertia and uncertainty
346 on optimal CO₂-emission abatement. *Nature*, 390(6657):270–273, Nov. 1997. ISSN 0028-0836, 1476-
347 4687. doi: 10.1038/36825. URL <http://www.nature.com/articles/36825>.
- 348 C. Hambel, H. Kraft, and E. Schwartz. Optimal carbon abatement in a stochastic equilibrium
349 model with climate change. *European Economic Review*, 132:103642, Feb. 2021. ISSN 00142921.
350 doi: 10.1016/j.eurocorev.2020.103642. URL <https://linkinghub.elsevier.com/retrieve/pii/S0014292120302725>.
- 352 W. W. Hogan and D. W. Jorgenson. Productivity trends and the cost of reducing CO₂ emissions. *The*
353 *Energy Journal*, 12(1):67–85, 1991. URL <https://www.jstor.org/stable/41322403>.
- 354 C. Hope, J. Anderson, and P. Wenman. Policy analysis of the greenhouse effect. *Energy Policy*,
355 21(3):327–338, Mar. 1993. ISSN 03014215. doi: 10.1016/0301-4215(93)90253-C. URL <https://linkinghub.elsevier.com/retrieve/pii/030142159390253C>.
- 357 P. H. Howard and T. Sterner. Few and Not So Far Between: A Meta-analysis of Climate Dam-
358 age Estimates. *Environmental and Resource Economics*, 68(1):197–225, Sept. 2017. ISSN 0924-
359 6460, 1573-1502. doi: 10.1007/s10640-017-0166-z. URL <http://link.springer.com/10.1007/s10640-017-0166-z>.
- 361 Intergovernmental Panel on Climate Change. Climate change 2021: The physical science basis. 2021.
362 URL https://report.ipcc.ch/ar6wg1/pdf/IPCC_AR6_WGI_FinalDraft_FullReport.pdf.

- 363 Intergovernmental Panel on Climate Change. Climate change 2022: Impacts, adaptation, and
364 vulnerability. 2022. URL https://report.ipcc.ch/ar6wg2/pdf/IPCC_AR6_WGII_FinalDraft_FullReport.pdf.
- 366 F. Joos, R. Roth, J. S. Fuglestvedt, G. P. Peters, I. G. Enting, W. von Bloh, V. Brovkin, E. J.
367 Burke, M. Eby, N. R. Edwards, T. Friedrich, T. L. Frölicher, P. R. Halloran, P. B. Holden,
368 C. Jones, T. Kleinen, F. T. Mackenzie, K. Matsumoto, M. Meinshausen, G.-K. Plattner, A. Reisinger,
369 J. Segschneider, G. Shaffer, M. Steinacher, K. Strassmann, K. Tanaka, A. Timmermann, and A. J.
370 Weaver. Carbon dioxide and climate impulse response functions for the computation of green-
371 house gas metrics: a multi-model analysis. *Atmospheric Chemistry and Physics*, 13(5):2793–2825,
372 Mar. 2013. ISSN 1680-7324. doi: 10.5194/acp-13-2793-2013. URL <https://acp.copernicus.org/articles/13/2793/2013/>.
- 374 D. W. Jorgenson. *Double dividend: environmental taxes and fiscal reform in the United States*. MIT
375 Press, Cambridge, MA, 2013. ISBN 9780262027090.
- 376 D. Lemoine. The Climate Risk Premium: How Uncertainty Affects the Social Cost of Carbon. *Journal
377 of the Association of Environmental and Resource Economists*, 8(1):27–57, Jan. 2021. ISSN 2333-
378 5955, 2333-5963. doi: 10.1086/710667. URL <https://www.journals.uchicago.edu/doi/10.1086/710667>.
- 380 D. Lemoine and C. P. Traeger. Ambiguous tipping points. *Journal of Economic Behavior &
381 Organization*, 132:5–18, Dec. 2016a. ISSN 01672681. doi: 10.1016/j.jebo.2016.03.009. URL
382 <https://linkinghub.elsevier.com/retrieve/pii/S0167268116300221>.
- 383 D. Lemoine and C. P. Traeger. Economics of tipping the climate dominoes. *Nature Climate Change*,
384 6(5):514–519, May 2016b. ISSN 1758-678X, 1758-6798. doi: 10.1038/nclimate2902. URL <https://www.nature.com/articles/nclimate2902>.
- 386 R. E. Lucas. Asset Prices in an Exchange Economy. *Econometrica*, 46(6):1429–1445, 1978. ISSN
387 0012-9682. doi: 10.2307/1913837. URL <https://www.jstor.org/stable/1913837>.
- 388 N. G. Mankiw, M. Weinzierl, and D. Yagan. Optimal Taxation in Theory and Practice. *Journal of
389 Economic Perspectives*, 23(4):147–174, Nov. 2009. ISSN 0895-3309. doi: 10.1257/jep.23.4.147. URL
390 <https://pubs.aeaweb.org/doi/10.1257/jep.23.4.147>.
- 391 F. C. Moore and D. B. Diaz. Temperature impacts on economic growth warrant stringent mitigation
392 policy. *Nature Climate Change*, 5(2):127–131, Feb. 2015. ISSN 1758-678X, 1758-6798. doi: 10.1038/
393 nclimate2481. URL <http://www.nature.com/articles/nclimate2481>.
- 394 W. D. Nordhaus. An Optimal Transition Path for Controlling Greenhouse Gases. *Science*, 258(5086):
395 1315–1319, Nov. 1992. ISSN 0036-8075, 1095-9203. doi: 10.1126/science.258.5086.1315. URL <https://www.sciencemag.org/lookup/doi/10.1126/science.258.5086.1315>.
- 397 W. D. Nordhaus. Revisiting the social cost of carbon. *Proceedings of the National Academy of Sciences*,
398 114(7):1518–1523, Feb. 2017. ISSN 0027-8424, 1091-6490. doi: 10.1073/pnas.1609244114. URL
399 <https://pnas.org/doi/full/10.1073/pnas.1609244114>.
- 400 R. G. Richels and G. J. Blanford. The value of technological advance in decarbonizing the U.S. economy.
401 *Energy Economics*, 30(6):2930–2946, Nov. 2008. ISSN 01409883. doi: 10.1016/j.eneco.2008.06.005.
402 URL <https://linkinghub.elsevier.com/retrieve/pii/S014098830800087X>.
- 403 S. K. Rose, D. B. Diaz, and G. J. Blanford. Understanding the Social Cost of Carbon: A Model Di-
404 agnostic and Inter-comparison Study. *Climate Change Economics*, 08(02):1750009, May 2017. ISSN
405 2010-0078, 2010-0086. doi: 10.1142/S2010007817500099. URL <https://www.worldscientific.com/doi/abs/10.1142/S2010007817500099>.

- 407 R. Tol. Safe policies in an uncertain climate: an application of FUND. *Global Environmental Change*,
408 9(3):221–232, Oct. 1999. ISSN 09593780. doi: 10.1016/S0959-3780(99)00011-4. URL <https://linkinghub.elsevier.com/retrieve/pii/S0959378099000114>.
- 410 T. S. Van Den Bremer and F. Van Der Ploeg. The Risk-Adjusted Carbon Price. *American Economic
411 Review*, 111(9):2782–2810, Sept. 2021. ISSN 0002-8282. doi: 10.1257/aer.20180517. URL <https://pubs.aeaweb.org/doi/10.1257/aer.20180517>.
- 413 A. Vogt-Schilb, G. Meunier, and S. Hallegatte. When starting with the most expensive option makes
414 sense: Optimal timing, cost and sectoral allocation of abatement investment. *Journal of Environ-
415 mental Economics and Management*, 88:210–233, Mar. 2018. ISSN 00950696. doi: 10.1016/j.jeem.
416 2017.12.001. URL <https://linkinghub.elsevier.com/retrieve/pii/S0095069617308392>.